Coalescing binary systems of compact objects to (post)$^{5/2}$-Newtonian order. V. Spin effects

Lawrence E. Kidder *

McDonnell Center for the Space Sciences, Department of Physics, Washington University, St. Louis, Missouri 63130
(Received 19 January 1995)

We examine the effects of spin-orbit and spin-spin couplings on the inspiral of a coalescing binary system of spinning compact objects and on the gravitational radiation emitted therefrom. Using a formalism developed by Blanchet, Damour, and Iyer we calculate the contributions due to the spins of the bodies to the symmetric trace-free radiative multipole moments which are used to calculate the waveform, energy loss, and angular momentum loss from the inspiraling binary. Using equations of motion which include terms due to spin-orbit and spin-spin couplings, we evolve the orbit of a coalescing binary and use the orbit to calculate the emitted gravitational waveform. We find the spins of the bodies affect the waveform in several ways: (1) the spin terms contribute to the orbital decay of the binary, and thus to the accumulated phase of the gravitational waveform; (2) the spins cause the orbital plane to precess, which changes the orientation of the orbital plane with respect to an observer, thus causing the shape of the waveform to be modulated; (3) the spins contribute directly to the amplitude of the waveform. We discuss the size and importance of spin effects for the case of two coalescing neutron stars, and for the case of a neutron star orbiting a rapidly rotating $10 M_\odot$ black hole.

PACS number(s): 04.25.Nx, 04.30.−w, 04.80.Nn, 97.80.Fk

I. INTRODUCTION AND SUMMARY

Coalescing binary systems of compact objects are the most promising source of gravitational waves which could be detected by laser interferometric gravitational wave detectors such as the currently funded U.S. Laser Interferometric Gravitational Wave Observatory (LIGO) and French-Italian VIRGO detector [1]. These systems consist of neutron stars or black holes whose orbits decay because of the dissipative effect of gravitational radiation. The binary pulsar PSR 1913+16 is an example of such a system and has given us our first evidence that gravitational waves exist [2]. Laser interferometric gravitational wave detectors will be able to observe the very late stages of the inspiral of coalescing binaries (typically the final several minutes) as the gravitational wave frequency sweeps through a detector's bandwidth from 10 Hz to 1000 Hz.

In the previous papers in this series [3–6] we have studied the evolution of coalescing binary systems using a post-Newtonian approximation. The post-Newtonian approximation involves an expansion of corrections to Newtonian gravitational theory with an expansion parameter $\epsilon \approx v^2 \approx m/r$, which is assumed to be small (we use units in which $G = c = 1$), where $m = m_1 + m_2$ denotes the total mass of the system, and where r and v are the orbital separation and velocity. Since we are interested in the late stages of the inspiral, where the fields may not be so

small and the velocity not so slow, we use an expansion carried out to the highest practical order. We use equations of motion carried out to (post)$^{5/2}$-Newtonian order, the order at which the dominant gravitational radiation-reaction damping forces occur. Schematically the equations of motion are given as

$$d^2\mathbf{x}/dt^2 = -(m\mathbf{x}/r^3)[1 + O(\epsilon) + O(\epsilon^{3/2}) + O(\epsilon^2) + O(\epsilon^{5/2}) + \cdots], \qquad (1.1)$$

where $\mathbf{x} = \mathbf{x_1} - \mathbf{x_2}$ denotes the separation vector between the bodies and $r = |\mathbf{x}|$. We use a gravitational waveform carried out to (post)$^{3/2}$-Newtonian order beyond the quadrupole formula. Schematically,

$$h^{ij} = \frac{2}{D}\left[Q^{ij}\left\{1 + O(\epsilon^{1/2}) + O(\epsilon) + O(\epsilon^{3/2}) + \cdots\right\}\right]_{\text{TT}}, \qquad (1.2)$$

where Q^{ij} represents the usual quadrupole term (two time derivatives of the mass quadrupole moment tensor), D is the distance between the source and an observer, and TT denotes that the transverse traceless part of the tensor should be taken [(post)^2-Newtonian contributions have recently been derived by Blanchet *et al.* [7]]. Given a set of initial conditions, we evolve the orbit with the equations of motion and calculate the emitted gravitational radiation. In previous papers we ignored the effects on the motion and radiation due to the spins of the bodies. It is the purpose of this paper to take these effects into account.

The contribution of the spins of the bodies to the equations of motion has been studied by numerous authors

---

*Present address: Department of Physics and Astronomy, Northwestern University, Evanston, Illinois 60208.

[8–11]. They include a contribution due to a spin-orbit interaction and a contribution due to a spin-spin interaction. In Sec. II we write down the spin-orbit and spin-spin contributions to the equations of motion and show that, although they are formally post-Newtonian corrections to the equations of motion, for compact bodies they are effectively (post)$^{3/2}$-Newtonian and (post)^2-Newtonian corrections, respectively, in part because they involve factors of order (R/r) where R is the size of the body which is on the order of m for a compact body. We add these contributions to our previous equations of motion, and obtain equations of motion valid for arbitrary masses and spins. Our equations of motion neglect tidal effects; for compact binary systems these effects are expected to be very small until the very late stages of inspiral [3,12]. We also ignore rotationally induced quadrupole effects which would enter at the same order as spin-spin effects; these also are expected to be small until very late stages, except possibly for very rapidly rotating Kerr black holes [12]. The major effect of the spins on the orbital evolution is that they cause the orbital plane to precess, thus changing its orientation in space. The spins themselves also precess; the precession equations are also written down in Sec. II.

Recently, we calculated the spin contributions to the symmetric trace-free radiative multipole moments which we used to calculate the spin contributions to the energy lost from a binary system due to the gravitational radiation emitted from the system [13]. In Sec. III we present the details of that calculation, and calculate the spin contributions to the gravitational waveform, the an-gular momentum lost from the system, and the linear momentum ejected from the system.

Since the emission of gravitational radiation tends to circularize the orbits of the binary system [3], we study the system under the assumption of circular orbits. This assumption should hold until the very late stages of inspiral when either the bodies start to merge, tidal effects become important, or the innermost stable circular orbit is reached in which case the system undergoes a transition from inspiral to plunge [5,14]. Assuming circular orbits, we calculate the spin-orbit and spin-spin contributions to the energy loss and variation of the orbital frequency, and hence to corrections in the accumulated orbital phase. In Table I we compare these contributions to the analogous contributions due to the quadrupole term and other post-Newtonian terms for various binary systems. These contributions to the orbital phase are important since, in order to extract information from the observed waveforms, theoretical templates must match the observed waveform to within about one cycle (which corresponds to half an orbit) over the several hundred cycles that appear in the sensitive region of a detector's bandwidth (between roughly 40 Hz and 100 Hz). Note that the templates do not have to match the observed waveform within one cycle over the entire bandwidth from 10 Hz to 1000 Hz (as suggested by Cutler et al. [15]) since the detector is more sensitive to the signal at some frequencies than in others [16]. As seen in Fig. 2 of Ref. [17], 60% of the signal to noise from a binary inspiral will accumulate between 40 Hz and 100 Hz due to the shape of the LIGO noise spectrum, and to the fact that there are more orbits

TABLE I. The contributions to the number of orbits for an inspiraling binary system which is in a LIGO-type detector's bandwidth, from quadrupole (Quad), post-Newtonian (PN), tail, spin-orbit (SO), and spin-spin (SS) terms. Masses are in units of $M_\odot$. In the first table, the observed inspiral begins when the gravitational wave frequency enters the bandwidth at the seismic cutoff around 10 Hz, and is cut off when either the quadrupole radiation of the binary has left the detector's bandwidth (at around 1000 Hz), or when the binary reaches its innermost stable circular orbit at which point the binary will plunge to a single object in one or two orbits. In the second table, we list the contribution to the number of orbits in the narrower bandwidth of 40 Hz to 100 Hz. The spin contributions shown are the maximum contributions assuming the bodies are maximally spinning ($\chi = \chi_{max}$). The magnitude and sign of the spin contributions depend on the specific orientations of the spins with respect to the orbital plane.

m_1	m_2	$r_{10\ Hz}/m$	f_{cut} (Hz)	r_{cut}/m	Quad	PN	Tail	SO	SS
1.4	1.4	174	1000	7.3	8015	219	-104	±44	±1.2
0.9	1.8	178	1000	7.5	9581	249	-119	±53	±1.2
0.5	2.0	187	1000	7.5	15128	351	-175	±82	±1.3
1.4	10	68	345	5.6	1787	106	-90	±63	±1.0
1.4	100	15	42	5.1	337	66	-112	±83	±0.3
10	10	46	183	6.0	300	29	-25	±15	±1.0
5	10	56	245	6.0	547	43	-35	±22	±1.2

m_1	m_2	$r_{40\ Hz}/m$	$r_{100\ Hz}/m$	Quad	PN	Tail	SO	SS
1.4	1.4	68	37	623	33	-19	±12	±0.5
0.9	1.8	70	38	745	37	-22	±14	±0.5
0.5	2.0	74	39	1175	531	-33	±22	±0.6
1.4	10	26	14	139	16	-18	±13	±0.3
10	10	18	9.3	24	4.7	-5.3	±3.3	±0.3
5	10	22	11	43	6.8	-7.3	±4.6	±0.3

at lower frequencies. In Table I we list the orbital phase contributions for both the restricted bandwidth (40–100 Hz) and the entire bandwidth (10–1000 Hz) of a LIGO-type detector. We see that the spin-orbit correction to the accumulated orbital phase is important (unless the spins are very small), while the spin-spin contribution is negligible unless rapidly rotating black holes are present. Note that the contributions of the post-Newtonian terms are less important in the narrower bandwidth than in the entire bandwidth since the sensitive region of the bandwidth is at low frequencies, for which post-Newtonian corrections are less important in most systems. Conversely, the use of matched templates may allow estimations of spins via the spin-orbit terms [13,15].

Using the equations of motion and the equations of precession, we numerically evolve the orbit for a binary system of arbitrary masses and spins. Using the orbit we are then able to calculate the gravitational waveform emitted by the system. If the spins of the bodies are not aligned perpendicular to the orbital plane, the orbital plane will precess in space thus changing its orientation with respect to an observer. Since an observed gravitational waveform depends upon the orientation of the orbital plane with respect to the observer, this precession will cause the waveform to be modulated. Figure 1 shows an example of this modulation. We see that these modu-

lations depend significantly upon the observer's location with respect to the source, and upon the orientation of the detector relative to the incoming wave. The size of the modulations also depends upon the relative magnitudes of the orbital angular momentum $\mathbf{L}$ and the total spin $\mathbf{S}$ and upon their relative orientation. (See Fig. 2 for a description of the source coordinate system.) If the angle between $\mathbf{L}$ and $\mathbf{S}$ is small, the modulations of the waveform will be small. If $|\mathbf{S}| \ll |\mathbf{L}|$, then the modulations are small regardless of their relative orientation. For a circular orbit $|\mathbf{L}| = \mu(rm)^{1/2}$ to leading order, while for each spin we define $|\mathbf{S_A}| = \chi_A m_A^2$ where $0 \leq \chi_A \leq \chi_{max}$, where $\chi_{max} = 1$ for a black hole and depends on the uncertain nuclear equation of state for neutron stars. For most neutron star models $\chi_{max} \leq 0.7$ [18]. In Fig. 3 we compare the relative sizes of $\mathbf{L}$ and $\mathbf{S}$ for the case of equal masses and for the case of a 10:1 mass ratio. We see that $|\mathbf{S}| \ll |\mathbf{L}|$ almost always for the equal mass case, so that the modulations of the waveform will be small. For a neutron star orbiting a rapidly rotating massive black hole, however, the modulations can be substantial if $\mathbf{L}$ and $\mathbf{S}$ are sufficiently misaligned. The modulation of the waveform due to the spin-induced orbital precession has also been independently studied by Apostolatos et al. [19].

There is also an explicit contribution to the waveform due to radiative multipole moments generated by the spins of the bodies. This contribution is relatively small until the late stages of inspiral. In Fig. 4 we compare the spin-orbit and spin-spin contributions to the waveform with the quadrupole contribution and higher-order post-Newtonian contributions for the last few orbits before coalescence. We see that the spin-orbit contribution
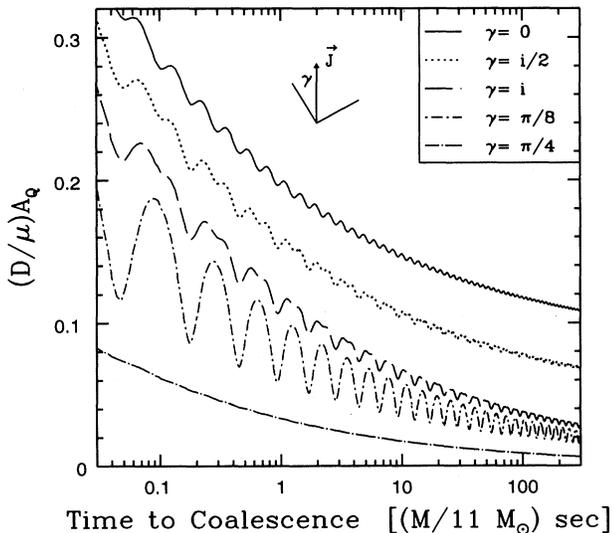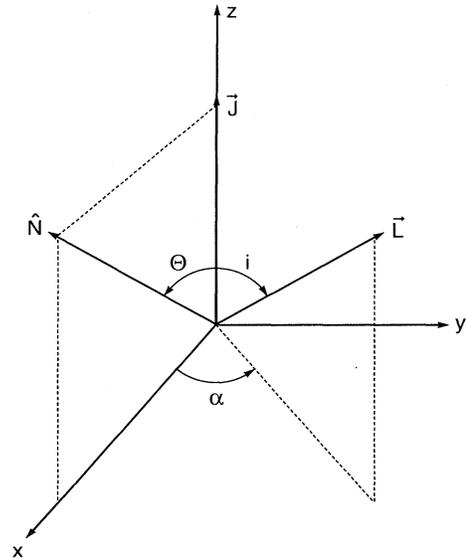

FIG. 1. Amplitude modulation of gravitational waveforms by spin-induced orbital precession, plotted against time to coalescence. System consists of a nonspinning $1M_\odot$ neutron star and a maximally spinning black hole of $10M_\odot$. Spin and orbital angular momentum vectors are initially misaligned by $11.3°$. Initial orbital inclination relative to $\mathbf{J}$ is i. The angle γ represents the orientation of the detector relative to $\mathbf{J}$, with the detector located on the x axis (see Fig. 2) such that the source is directly overhead. Curves show envelope of the quadrupole waveform for various detector orientations (The curves for the cases $\gamma = 0$, $i/2$, and i would lie on top of one another, and so the first two have been shifted upward for ease of presentation). Gravitational-wave frequency runs from 10 Hz on the right to 300 Hz on the left.

FIG. 2. The source coordinate system. The total angular momentum $\mathbf{J}$ initially lies along the z axis. The detector is located in the x-z plane. The spherical angles (i, α) define the direction of the Newtonian angular momentum $\mathbf{L_N}$ which is perpendicular to the orbital plane. In terms of celestial mechanics, the angle of ascending nodes is $\alpha + \pi/2$.
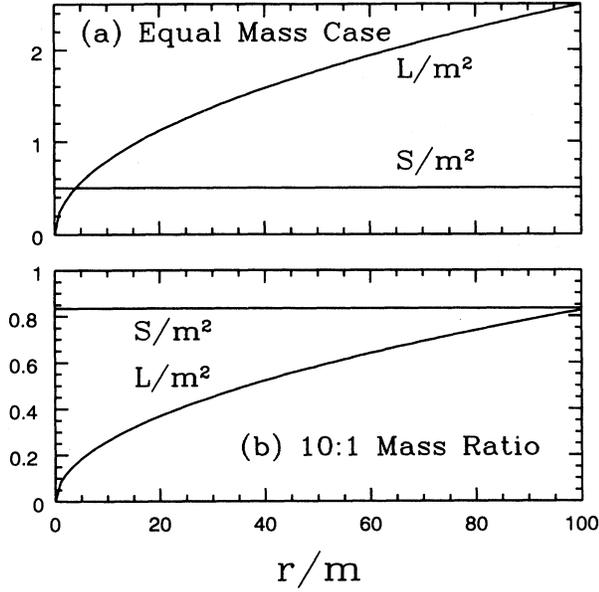
FIG. 3. A comparison of the magnitudes of the orbital angular momentum and spin angular momentum as the binary inspirals. (a) The equal mass case (assuming the bodies are maximally spinning). (b) The case of a 10:1 mass ratio.

is comparable to the higher-order post-Newtonian contributions, while the spin-spin contribution is practically negligible.

The rest of the paper presents the details. In Sec. II we assemble the equations necessary to evolve the orbit. In Sec. III we derive the spin corrections to the radiative multipoles, and calculate the spin corrections to the gravitational radiation emitted, energy lost, angular momentum lost, and linear momentum ejected from the binary system. In Sec. IV we examine the system in the limit of circular orbits, and in the limit of small precessions. In Sec. V we present our results for various numerically evolved orbits. Finally, in Sec. VI we discuss these results, and their implications for extracting useful information from observations. In Appendix A we discuss the issue of "spin supplementary conditions" used to fix the center of mass of the spinning bodies to post-Newtonian order. In Appendix B we list the post-Newtonian corrections to the circular orbit waveform. In Appendix C we compare our results with calculations involving test masses orbiting spinning black holes.
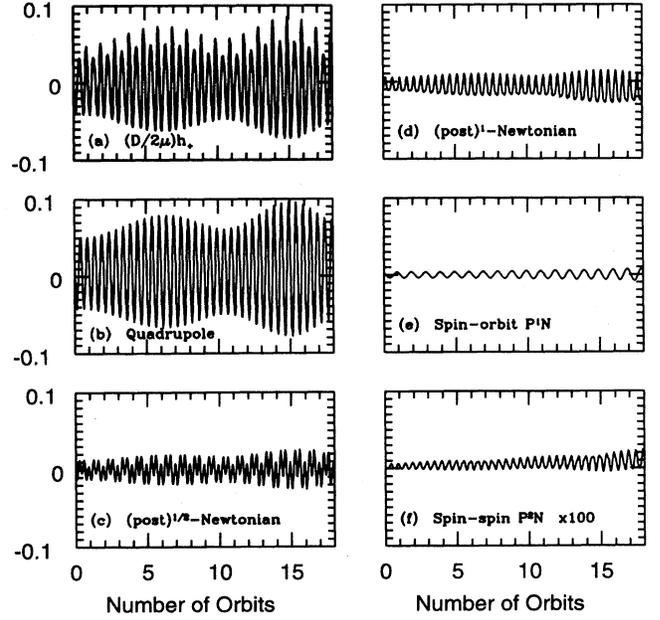

FIG. 4. Gravitational waveform plotted against orbital phase for a 10:1.4 mass-ratio system. The smaller body's spin is aligned with the orbital angular momentum $\mathbf{L}$, while the larger body's spin is tilted by an angle of 30° with respect to $\mathbf{L}$. Plotted is $(D/2\mu)h_+$ for an observer at $\Theta = 90°$. Plots begin at an orbital separation of $15m$ and terminate at $10m$. (a) The total waveform. (b) The quadrupole contribution to the waveform. (c) The first higher-order post-Newtonian correction $[O(\epsilon^{1/2})$ beyond the quadrupole]. (d) The next post-Newtonian correction. (e) The leading-order spin-orbit contribution to the waveform. (f) The leading-order spin-spin contribution to the waveform (note the different scale). Notice the modulation due to the precession of the orbital plane.

II. ORBITAL EVOLUTION EQUATIONS

A. Equations of motion

Equations of motion for two bodies of arbitrary mass and spin have been developed by numerous authors (for reviews and references see [8–11]). By eliminating the center of mass of the system, we convert the two-body equations of motion to a relative one-body equation of motion given by

$$\mathbf{a} = \mathbf{a}_N + \mathbf{a}_{PN} + \mathbf{a}_{SO} + \mathbf{a}_{2PN} + \mathbf{a}_{SS} + \mathbf{a}_{RR}, \qquad (2.1)$$

where

$$\mathbf{a}_N = -\frac{m}{r^2}\hat{\mathbf{n}}, \qquad (2.2a)$$

$$\mathbf{a}_{PN} = -\frac{m}{r^2}\left\{\hat{\mathbf{n}}\left[(1+3\eta)v^2 - 2(2+\eta)\frac{m}{r} - \frac{3}{2}\eta\dot{r}^2\right] - 2(2-\eta)\dot{r}\mathbf{v}\right\}, \qquad (2.2b)$$

$$\mathbf{a}_{SO} = \frac{1}{r^3}\left\{6\hat{\mathbf{n}}\left[(\hat{\mathbf{n}}\times\mathbf{v})\cdot\left(2\mathbf{S}+\frac{\delta m}{m}\mathbf{\Delta}\right)\right] - \left[\mathbf{v}\times\left(7\mathbf{S}+3\frac{\delta m}{m}\mathbf{\Delta}\right)\right] + 3\dot{r}\left[\hat{\mathbf{n}}\times\left(3\mathbf{S}+\frac{\delta m}{m}\mathbf{\Delta}\right)\right]\right\}, \qquad (2.2c)$$

$$\mathbf{a}_{2\text{PN}} = -\frac{m}{r^2}\left\{\hat{\mathbf{n}}\left[\frac{3}{4}(12+29\eta)\left(\frac{m}{r}\right)^2 + \eta(3-4\eta)v^4 + \frac{15}{8}\eta(1-3\eta)\dot{r}^4\right.\right.$$

$$\left. - \frac{3}{2}\eta(3-4\eta)v^2\dot{r}^2 - \frac{1}{2}\eta(13-4\eta)\frac{m}{r}v^2 - (2+25\eta+2\eta^2)\frac{m}{r}\dot{r}^2\right]$$

$$\left. - \frac{1}{2}\dot{r}\mathbf{v}\left[\eta(15+4\eta)v^2 - (4+41\eta+8\eta^2)\frac{m}{r} - 3\eta(3+2\eta)\dot{r}^2\right]\right\}, \tag{2.2d}$$

$$\mathbf{a}_{\text{SS}} = -\frac{3}{\mu r^4}\{\hat{\mathbf{n}}(\mathbf{S}_1\cdot\mathbf{S}_2) + \mathbf{S}_1(\hat{\mathbf{n}}\cdot\mathbf{S}_2) + \mathbf{S}_2(\hat{\mathbf{n}}\cdot\mathbf{S}_1) - 5\hat{\mathbf{n}}(\hat{\mathbf{n}}\cdot\mathbf{S}_1)(\hat{\mathbf{n}}\cdot\mathbf{S}_2)\}, \tag{2.2e}$$

$$\mathbf{a}_{\text{RR}} = \frac{8}{5}\eta\frac{m^2}{r^3}\left\{\dot{r}\hat{\mathbf{n}}\left[18v^2 + \frac{2}{3}\frac{m}{r} - 25\dot{r}^2\right] - \mathbf{v}\left[6v^2 - 2\frac{m}{r} - 15\dot{r}^2\right]\right\}, \tag{2.2f}$$

where $\mathbf{a}_N$, $\mathbf{a}_{\text{PN}}$, and $\mathbf{a}_{2\text{PN}}$ are the Newtonian, (post)^1-Newtonian, and (post)^2-Newtonian contributions to the equations of motion, $\mathbf{a}_{\text{RR}}$ is the contribution to the equation of motion due to the radiation-reaction force, and $\mathbf{a}_{\text{SO}}$ and $\mathbf{a}_{\text{SS}}$ are the spin-orbit and spin-spin contributions to the equations of motion which we have ignored previously, and where $\mathbf{x} \equiv \mathbf{x}_1 - \mathbf{x}_2$, $\mathbf{v} = d\mathbf{x}/dt$, $\hat{\mathbf{n}} \equiv \mathbf{x}/r$, $\mu \equiv m_1 m_2/m$, $\eta \equiv \mu/m$, $\delta m \equiv m_1 - m_2$, $\mathbf{S} \equiv \mathbf{S}_1 + \mathbf{S}_2$, and $\boldsymbol{\Delta} \equiv m(\mathbf{S}_2/m_2 - \mathbf{S}_1/m_1)$, and an overdot denotes d/dt.

It should be noted that the above expression for $\mathbf{a}_{\text{SO}}$ is not unique; it depends on a "spin supplementary condition" (SSC) which is related to the definition of the center-of-mass world line x_A^μ for each body A. The above form of $\mathbf{a}_{\text{SO}}$ is for the covariant SSC given by $S_A^{\mu\nu}u_{A\nu} = 0$, where u_A^μ is the four-velocity of the center-of-mass world line of body A, and

$$S_A^{\mu\nu} \equiv 2\int_A (x^{[\mu} - x_A^{[\mu})\tau^{\nu]0}d^3x, \tag{2.3}$$

where $\tau^{\mu\nu}$ denotes the stress-energy tensor of matter plus gravitational fields satisfying $\tau^{\mu\nu}{}_{,\nu} = 0$, and square brackets around indices denote antisymmetrization. Note that the spin vector $\mathbf{S}$ of each body is defined by $S_A^i = \frac{1}{2}\epsilon_{ijk}S_A^{jk}$. We discuss the issue of SSC's in more detail in Appendix A. Here we simply wish to emphasize that since we have chosen a center-of-mass world line for each body through our choice of a SSC, we must ensure that all our calculations are consistent with this choice.

Since the spin of each body is of order $mR_A\bar{v}_A$ where R_A is the size of body A and $\bar{v}_A$ is its rotational velocity, we see that the spin-orbit and spin-spin accelerations are of order $(R_A/r)v\bar{v}_A$ and $(R_A/r)^2\bar{v}_A^2$, respectively, compared to the Newtonian acceleration; these terms thus are formally of (post)^1-Newtonian order. For compact objects, however, R_A is of order m, while $\bar{v}_A$ could be of order unity for sufficiently rapid rotation, so that the spin-orbit and spin-spin accelerations are effectively of (post)$^{3/2}$-Newtonian and (post)^2-Newtonian order, respectively. If the bodies are slowly rotating, the spin contributions to the acceleration will be even smaller.

It is interesting to note that while $\mathbf{a}_N$, $\mathbf{a}_{\text{PN}}$, $\mathbf{a}_{2\text{PN}}$, and $\mathbf{a}_{\text{RR}}$ are all confined to the orbital plane, in general $\mathbf{a}_{\text{SO}}$ and $\mathbf{a}_{\text{SS}}$ are not. As a result, the orbital plane will precess in space (except for specific spin orientations) resulting in modulations of the observed waveform. We will discuss this effect in more detail in Sec. IV. Iyer and Will [20] have derived post-Newtonian corrections to $\mathbf{a}_{\text{RR}}$ at $O(\epsilon^{7/2})$ and $O(\epsilon^4)$ where the latter are the spin-orbit corrections to radiation reaction.

B. Spin precession equations

In addition to the precession of the orbital plane, there are precessions of the spin vectors themselves. This effect has been studied by numerous authors [8–10]; the relevant equations are

$$\dot{\mathbf{S}}_1 = \frac{1}{r^3}\left\{(\mathbf{L}_N \times \mathbf{S}_1)\left(2 + \frac{3}{2}\frac{m_2}{m_1}\right) - \mathbf{S}_2 \times \mathbf{S}_1\right.$$

$$\left. + 3(\hat{\mathbf{n}}\cdot\mathbf{S}_2)\hat{\mathbf{n}}\times\mathbf{S}_1\right\}, \tag{2.4a}$$

$$\dot{\mathbf{S}}_2 = \frac{1}{r^3}\left\{(\mathbf{L}_N \times \mathbf{S}_2)\left(2 + \frac{3}{2}\frac{m_1}{m_2}\right) - \mathbf{S}_1 \times \mathbf{S}_2\right.$$

$$\left. + 3(\hat{\mathbf{n}}\cdot\mathbf{S}_1)\hat{\mathbf{n}}\times\mathbf{S}_2\right\}, \tag{2.4b}$$

where $\mathbf{L}_N \equiv \mu(\mathbf{x}\times\mathbf{v})$ is the Newtonian orbital angular momentum, and where the first term in each expression is the precession due to spin-orbit coupling, while the second and third terms are due to spin-spin coupling. It is straightforward to show that the total spin $\mathbf{S}$ evolves as

$$\dot{\mathbf{S}} = \frac{1}{r^3}\left\{\left[\mathbf{L}_N \times \left(\frac{7}{2}\mathbf{S} + \frac{3}{2}\frac{\delta m}{m}\boldsymbol{\Delta}\right)\right] + 3(\hat{\mathbf{n}}\cdot\mathbf{S}_1)(\hat{\mathbf{n}}\times\mathbf{S}_2)\right.$$

$$\left. + 3(\hat{\mathbf{n}}\cdot\mathbf{S}_2)(\hat{\mathbf{n}}\times\mathbf{S}_1)\right\}. \tag{2.5}$$

It is useful to note that the precession of spins is a post-Newtonian effect, since $L_N/r^3 \approx (v/r)(\mu/r) \approx \epsilon(d/dt)$, and $S_i/r^3 \approx m_iR\bar{v}/r^3 \approx \epsilon^{3/2}(d/dt)$.

Since the precession equations have the form $\dot{\mathbf{S}}_A = \mathbf{\Omega}_A \times \mathbf{S}_A$, the magnitudes of the spins remain constant. The spin $\mathbf{S}_A$ instantaneously precesses about the vector $\mathbf{\Omega}_A$ with a precession frequency given by $\omega_p^{(A)} = |\mathbf{\Omega}_A|$. It is an instantaneous precession since $\mathbf{\Omega}_A$ is precessing itself in some complicated manner. Notice that if both bodies are spinning, the total spin $\mathbf{S}$ (with rare exceptions) does not have constant magnitude as the spins precess.

C. Constants of the motion

Through (post)^2-Newtonian order, the equations of motion can be derived from a generalized Lagrangian,

that is, a Lagrangian which is a function not just of the relative position and relative velocity, but also of the relative acceleration [21]. In our previous papers [5,13] we transformed the Lagrangian into relative coordinates and used it to compute the energy and total angular momentum of the system which are conserved to (post)^2-Newtonian order, in the absence of radiation reaction. Combining our expressions for the nonspinning case and the spinning case, the energy is given by

$$E = E_\mathrm{N} + E_\mathrm{PN} + E_\mathrm{SO} + E_\mathrm{2PN} + E_\mathrm{SS}, \qquad (2.6)$$

where

$$E_\mathrm{N} = \mu \left\{ \frac{1}{2}v^2 - \frac{m}{r} \right\}, \qquad (2.7a)$$

$$E_\mathrm{PN} = \mu \left\{ \frac{3}{8}(1 - 3\eta)v^4 + \frac{1}{2}(3 + \eta)v^2\frac{m}{r} + \frac{1}{2}\eta\frac{m}{r}\dot{r}^2 + \frac{1}{2}\left(\frac{m}{r}\right)^2 \right\}, \qquad (2.7b)$$

$$E_\mathrm{SO} = \frac{1}{r^3}\mathbf{L}_\mathrm{N} \cdot \left(\mathbf{S} + \frac{\delta m}{m}\mathbf{\Delta} \right), \qquad (2.7c)$$

$$\begin{aligned} E_\mathrm{2PN} = \mu \bigg\{ &\frac{5}{16}(1 - 7\eta + 13\eta^2)v^6 - \frac{3}{8}\eta(1 - 3\eta)\frac{m}{r}\dot{r}^4 + \frac{1}{8}(21 - 23\eta - 27\eta^2)\frac{m}{r}v^4 \\ &+ \frac{1}{8}(14 - 55\eta + 4\eta^2)\left(\frac{m}{r}\right)^2 v^2 + \frac{1}{4}\eta(1 - 15\eta)\frac{m}{r}v^2\dot{r}^2 - \frac{1}{4}(2 + 15\eta)\left(\frac{m}{r}\right)^3 \\ &+ \frac{1}{8}(4 + 69\eta + 12\eta^2)\left(\frac{m}{r}\right)^2\dot{r}^2 \bigg\}, \end{aligned} \qquad (2.7d)$$

$$E_\mathrm{SS} = \frac{1}{r^3}\left\{ 3(\hat{\mathbf{n}} \cdot \mathbf{S}_1)(\hat{\mathbf{n}} \cdot \mathbf{S}_2) - (\mathbf{S}_1 \cdot \mathbf{S}_2) \right\}, \qquad (2.7e)$$

and the total angular momentum is given by

$$\mathbf{J} = \mathbf{L} + \mathbf{S}, \qquad (2.8)$$

where

$$\mathbf{L} = \mathbf{L}_\mathrm{N} + \mathbf{L}_\mathrm{PN} + \mathbf{L}_\mathrm{SO} + \mathbf{L}_\mathrm{2PN}, \qquad (2.9a)$$

$$\mathbf{L}_\mathrm{PN} = \mathbf{L}_\mathrm{N}\left\{ \frac{1}{2}v^2(1 - 3\eta) + (3 + \eta)\frac{m}{r} \right\}, \qquad (2.9b)$$

$$\begin{aligned} \mathbf{L}_\mathrm{SO} = \frac{\mu}{m}\bigg\{ &\frac{m}{r}\hat{\mathbf{n}} \times \left[\hat{\mathbf{n}} \times \left(3\mathbf{S} + \frac{\delta m}{m}\mathbf{\Delta}\right)\right] \\ &- \frac{1}{2}\mathbf{v} \times \left[\mathbf{v} \times \left(\mathbf{S} + \frac{\delta m}{m}\mathbf{\Delta}\right)\right] \bigg\}, \end{aligned} \qquad (2.9c)$$

$$\begin{aligned} \mathbf{L}_\mathrm{2PN} = \mathbf{L}_\mathrm{N}\bigg\{ &\frac{3}{8}(1 - 7\eta + 13\eta^2)v^4 - \frac{1}{2}\eta(2 + 5\eta)\frac{m}{r}\dot{r}^2 \\ &+ \frac{1}{2}(7 - 10\eta - 9\eta^2)\frac{m}{r}v^2 \\ &+ \frac{1}{4}(14 - 41\eta + 4\eta^2)\left(\frac{m}{r}\right)^2 \bigg\}. \end{aligned} \qquad (2.9d)$$

Note that there is no spin-spin contribution to $\mathbf{J}$. It is straightforward to show that to (post)^2-Newtonian order, $\dot{E} = \dot{\mathbf{J}} = 0$, where it is understood that whenever the relative acceleration is found in the time derivative, the equation of motion carried to the appropriate order is substituted.

D. Precession of the orbital angular momentum

Since the total angular momentum $\mathbf{J}$ is conserved (in the absence of gravitational radiation), it is clear that the orbital angular momentum $\mathbf{L}$ must precess as

$$\dot{\mathbf{L}} = -\dot{\mathbf{S}}, \qquad (2.10)$$

where $\dot{\mathbf{S}}$ is given by Eq. (2.5).

If we restrict ourselves to the case of one spinning body, then

$$\dot{\mathbf{S}} = \frac{1}{r^3}\left\{ \frac{1}{2}\left(1 + 3\frac{m}{m_s}\right)\left(\mathbf{L}_\mathrm{N} \times \mathbf{S}\right) \right\}, \qquad (2.11)$$

where m_s is the mass of the spinning body. Since to

lowest order $\mathbf{J} = \mathbf{L_N} + \mathbf{S}$, then

$$\dot{\mathbf{S}} = \frac{1}{r^3}\left\{\frac{1}{2}(1+3\frac{m}{m_s})(\mathbf{J}\times\mathbf{S})\right\}. \qquad (2.12)$$

Similarly, since $\mathbf{L} = \mathbf{L_N}$ to lowest order,

$$\dot{\mathbf{L}} = \frac{1}{r^3}\left\{\frac{1}{2}(1+3\frac{m}{m_s})(\mathbf{J}\times\mathbf{L})\right\}. \qquad (2.13)$$

These two equations imply that $\mathbf{L}$ and $\mathbf{S}$ precess about the fixed vector $\mathbf{J}$ at the same rate with a precession frequency given by

$$\omega_p = \frac{|\mathbf{J}|}{2r^3}\left(1+3\frac{m}{m_s}\right). \qquad (2.14)$$

Note that $\mathbf{L_N}$ is not necessarily parallel to $\mathbf{L}$ because of the $\mathbf{L_{SO}}$ terms, so that the orbital plane (determined by $\mathbf{L_N}$) does not precess in the simple manner above. Instead the varying $\mathbf{L_{SO}}$ terms cause it to wobble slightly on an orbital timescale as it precesses about $\mathbf{J}$. This is illustrated in Fig. 5.

In the case of two spinning bodies $\mathbf{L}$, $\mathbf{S_1}$ and $\mathbf{S_2}$ precess in a very complicated manner (with few exceptions), which can only be examined numerically. Figure 6 shows an example of such a precession. Note that in this case the orbital plane tilts back and forth as it precesses about $\mathbf{J}$. In Sec. IV we will examine the precession of the spins and orbital angular momentum in the case of nearly circular orbits, and examine the effect of gravitational radiation on the simple precession for one spinning body, and on the more complicated case of two spinning bodies.
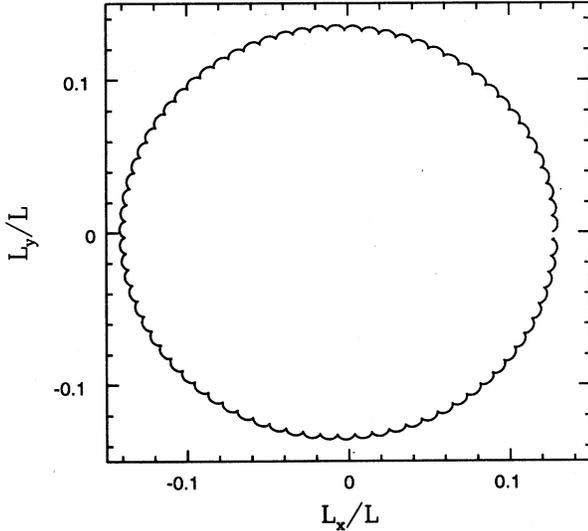

FIG. 5. The wobble of the orbital plane during simple precession (in the absence of gravitational-radiation damping). Plotted are the x and y components of the unit vector $\hat{\mathbf{L}}_N$ which defines the orbital plane. The total angular momentum $\mathbf{J}$ is directed out of the page. If the orbital plane were not wobbling as it precessed, the plot would be a circle whose radius depends on the inclination of the orbital plane with respect to $\mathbf{J}$.
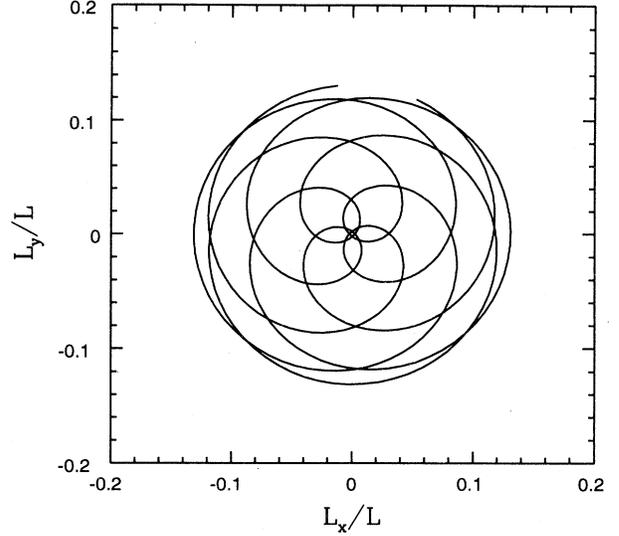

FIG. 6. The complicated precession of the orbital angular momentum $\mathbf{L}$ (in the absence of gravitational-radiation damping) for a 2:1 mass-ratio system with equal spins which are initially aligned in the orbital plane. Although the spins are equal, they precess at different rates so that at a later time they almost cancel one another. This leads to the tilting of the orbital plane as it precesses about $\mathbf{J}$. See Fig. 10 for the effects of gravitational radiation on the precession.

III. GRAVITATIONAL RADIATION EQUATIONS

A. Symmetric trace-free radiative multipoles

Our goal is to calculate the effects of the spins of the bodies on the gravitational radiation waveform emitted by the inspiraling binary and on the energy, angular momentum, and linear momentum radiated from the system. Thorne [22] showed that these quantities can be calculated using symmetric trace-free radiative multipole moments. For example the gravitational waveform to $(\text{post})^{3/2}$-Newtonian order is given by

$$h^{ij} = \frac{2}{D}\left\{\overset{(2)}{I^{ij}} + \frac{1}{3}\overset{(3)}{I^{ijk}}N^k + \frac{1}{12}\overset{(4)}{I^{ijkl}}N^kN^l\right.$$

$$+ \frac{1}{60}\overset{(5)}{I^{ijklm}}N^kN^lN^m + \cdots$$

$$+ \epsilon^{kl(i}\left[\frac{4}{3}\overset{(2)}{J^{j)k}}N^l + \frac{1}{2}\overset{(3)}{J^{j)km}}N^lN^m\right.$$

$$\left.\left. + \frac{2}{15}\overset{(4)}{J^{j)kmn}}N^lN^mN^n + \cdots\right]\right\}_{\text{TT}}, \qquad (3.1)$$

where $I^{ij\cdots}$ are the mass multipole moments (see below), $J^{ij\cdots}$ are the current multipole moments, D is the distance from the source to the observer, N^i is a unit vector from the center of mass of the source to the observation point, the notation (n) over each mul-

tipole moment denotes the number of derivatives with respect to retarded time, ϵ^{ijk} is the completely antisymmetric Levi-Civita symbol, and parentheses around indices denote symmetrization. To the accuracy we need, the mass quadrupole moment I^{ij} needs to be calculated to (post)$^{3/2}$-Newtonian order beyond the lowest order, the mass octopole moment I^{ijk} and current quadrupole moment J^{jk} need to be calculated to (post)^1-Newtonian order, I^{ijkl} and J^{jkm} need to be calculated to (post)$^{1/2}$-Newtonian order, and I^{ijklm} and J^{jkmn} need to be known only to lowest order.

Blanchet, Damour, and Iyer [23,24] (BDI) have developed a formalism for calculating these radiative multipole moments in terms of integrals over the source stress-energy. We use the BDI formalism to evaluate the spin-orbit and spin-spin corrections to the radiative multipole moments to the necessary order.

1. Mass multipole moments

The mass multipole moments in harmonic coordinates (the coordinates in which our equations of motion are written) are given to post-Newtonian order by Eq. (3.34) in Blanchet and Damour [23] as

$$I^L(u) = \int (x^L)^{\mathrm{STF}} \sigma(\mathbf{x}, u) d^3 x$$

$$- \frac{4(2l+1)}{(l+1)(2l+3)} \frac{d}{du} \int (x^{iL})^{\mathrm{STF}} \sigma^i(\mathbf{x}, u) d^3 x$$

$$+ \frac{1}{2(2l+3)} \frac{d^2}{du^2} \int |\mathbf{x}^2| (x^L)^{\mathrm{STF}} \sigma(\mathbf{x}, u) d^3 x,$$

$$(3.2)$$

where L denotes a multi-index (i.e., $x^L \equiv x^{i_1} x^{i_2} \cdots x^{i_l}$), the superscript STF denotes that only the symmetric trace-free part is to be taken, and the source densities are given by

$$\sigma(\mathbf{x}, t) = T^{00} + T^{ii}, \qquad (3.3a)$$

$$\sigma^i(\mathbf{x}, t) = T^{0i}. \qquad (3.3b)$$

In previous calculations involving nonspinning bodies we were able to evaluate the integrals by assuming a point particle limit. Taking into account the spins of the bodies, however, precludes this. Instead we will assume the bodies to be well-separated, approximately spherically symmetric (in harmonic coordinates), stationary, rigidly rotating compact objects whose structure is given by that of a perfect fluid. We will then neglect any effects due to the finite size of the bodies with the exception of each body's spin. The stress-energy tensor for a perfect fluid to the order we need is

$$T^{00} = \rho^* (1 + \Pi + \tfrac{1}{2} v^2 - U), \qquad (3.4a)$$

$$T^{0i} = \rho^* v^i, \qquad (3.4b)$$

$$T^{ij} = \rho^* v^i v^j + p \delta^{ij}, \qquad (3.4c)$$

where $\rho^* = \rho(1 + \tfrac{1}{2} v^2 + 3U)$ is the so-called "conserved density" (it satisfies a continuity equation to post-Newtonian order) [25], with ρ the local mass density, v the velocity, and U the Newtonian gravitational potential; Π is the specific internal energy density, and p is the pressure.

Substituting Eqs. (3.3) and (3.4) into Eq. (3.2) for the case $l = 2$, the mass quadrupole moment is given by

$$I^{ij} = \sum_A \left\{ \int_A (x^i x^j)^{\mathrm{STF}} \rho^*(\mathbf{x}) \left[1 + \frac{3}{2} v^2 - U + 3 \frac{p}{\rho^*(\mathbf{x})} \right. \right.$$

$$\left. + \Pi \right] d^3 x + \frac{1}{14} \frac{d^2}{dt^2} \int_A (x^i x^j)^{\mathrm{STF}} \mathbf{x}^2 \rho^*(\mathbf{x}) d^3 x$$

$$\left. - \frac{20}{21} \frac{d}{dt} \int_A (x^i x^j x^k)^{\mathrm{STF}} \rho^*(\mathbf{x}) v^k d^3 x \right\}. \qquad (3.5)$$

Following previous post-Newtonian calculations [4,26], we choose the following provisional definition for the center of mass for each body:

$$x_A^i = \frac{1}{m_A} \int_A x^i \rho^*(\mathbf{x}) \left[1 + \frac{1}{2} \bar{v}_A^2 + \Pi - \frac{1}{2} \bar{U}_A \right] d^3 x, \quad (3.6)$$

where

$$m_A = \int_A \rho^*(\mathbf{x}) \left[1 + \frac{1}{2} \bar{v}_A^2 + \Pi - \frac{1}{2} \bar{U}_A \right] d^3 x, \qquad (3.7)$$

where $\bar{v}_A^i = v^i - v_A^i$, $v_A^i = dx_A^i/dt$, and $\bar{U}_A$ is the Newtonian potential produced by the Ath body itself. It turns out that this definition of the center-of-mass world line does not correspond to the center-of-mass world line of our equations of motion chosen through the use of a SSC, but rather to one given by a different SSC. There does exist a transformation between the two world lines, given by [27]

$$x_A^i \longrightarrow x_A^i + \frac{1}{2m_A} (\mathbf{v}_A \times \mathbf{S}_A)^i . \qquad (3.8)$$

This shift in the world line is of post-Newtonian order, and so it can be neglected at lowest order. We choose to use our provisional definition of the center of mass to evaluate the integrals, and then use the transformation on the result so that it is consistent with our equations of motion. See Appendix A and Ref. [27] for more details.

Equation (3.5) has been evaluated by several authors [4,26] for the case of nonspinning bodies, i.e., $\bar{v}_A = 0$. By substituting $x^i = x_A^i + \bar{x}_A^i$ and $v^i = v_A^i + \bar{v}_A^i$ into Eq. (3.5), using the center-of-mass definition Eq. (3.6) and a virial theorem, and neglecting terms containing $\bar{x}_A^i \bar{x}_A^j$ which are $O(\beta^2)$ relative to $x_A^i x_A^j$ where $\beta \equiv R/r$, Blanchet and Schäfer [26] have rewritten Eq. (3.5) as

$$I^{ij} = \sum_A \left\{ m_A (x_A^i x_A^j)^{\text{STF}} \left[1 + \frac{3}{2} v_A^2 - \sum_{B \neq A} \frac{m_B}{r_{AB}} \right] - \frac{20}{21} \frac{d}{dt} \left[3 \int_A \rho^*(\mathbf{x}) \bar{v}_A^k (\bar{x}_A^i x_A^j x_A^k)^{\text{STF}} d^3 x \right. \right.$$

$$+ m_A (x_A^i x_A^j x_A^k)^{\text{STF}} v_A^k \right] + 6 v_A^k \int_A \rho^*(\mathbf{x}) (x_A^i \bar{x}_A^j)^{\text{STF}} \bar{v}_A^k d^3 x + \frac{1}{14} \frac{d^2}{dt^2} \left[m_A x_A^2 (x_A^i x_A^j)^{\text{STF}} \right]$$

$$+ \frac{1}{2} (x_A^i x_A^j)^{\text{STF}} \frac{d^2}{dt^2} \int_A \rho^*(\mathbf{x}) \bar{x}_A^2 d^3 x + 2 \int_A \rho^*(\mathbf{x}) (x_A^i \bar{x}_A^j)^{\text{STF}} \left[\bar{v}_A^2 - \frac{1}{2} \bar{U}_A + \frac{3p}{\rho^*(\mathbf{x})} \right] d^3 x \right\}. \tag{3.9}$$

The third integral in Eq. (3.9) is just the mass quadrupole moment of body A, which is of $O(\beta^2)$, and so we will neglect it. The last integral in Eq. (3.9) will also vanish because of our assumptions of approximate spherical symmetry and rigid rotation. This just leaves integrals of the type

$$\int_A \rho^*(\mathbf{x}) \bar{x}_A^a \bar{v}_A^b d^3 x = \int_A \rho^*(\mathbf{x}) \left\{ \bar{x}_A^{[a} \bar{v}_A^{b]} + \bar{x}_A^{(a} \bar{v}_A^{b)} \right\} d^3 x$$

$$= \frac{1}{2} S_A^{ab} + \frac{1}{2} \frac{d}{dt} \int_A \rho^*(\mathbf{x}) \bar{x}_A^a \bar{x}_A^b d^3 x,$$

where we have used Eq. (2.3) evaluated to lowest order. The second term on the right-hand side vanishes by our assumption of stationary spherical symmetry so we will neglect it. Changing the spin tensor to a spin vector we obtain

$$\int_A \rho^*(\mathbf{x}) \bar{x}_A^a \bar{v}_A^b d^3 x = \frac{1}{2} \epsilon^{iab} S_A^i. \tag{3.10}$$

Substituting Eq. (3.10) into Eq. (3.9) and carefully counting the STF parts we obtain

$$I^{ij} = \sum_A \left\{ m_A (x_A^i x_A^j)^{\text{STF}} \left[1 + \frac{3}{2} v_A^2 - \sum_{B \neq A} \frac{m_B}{r_{AB}} \right] - \frac{20}{21} \frac{d}{dt} \left[m_A (x_A^i x_A^j x_A^k)^{\text{STF}} v_A^k \right] \right.$$

$$+ \frac{1}{14} \frac{d^2}{dt^2} \left[m_A x_A^2 (x_A^i x_A^j)^{\text{STF}} \right] + 3 \left[x_A^i (\mathbf{v}_A \times \mathbf{S}_A)^j \right]^{\text{STF}} - \frac{4}{3} \frac{d}{dt} \left[x_A^i (\mathbf{x}_A \times \mathbf{S}_A)^j \right]^{\text{STF}} \right\}. \tag{3.11}$$

Using Eq. (3.8) so that we have a consistent center-of-mass definition with our equations of motion, the mass quadrupole moment becomes

$$I^{ij} = \sum_A \left\{ m_A (x_A^i x_A^j)^{\text{STF}} \left[1 + \frac{3}{2} v_A^2 - \sum_{B \neq A} \frac{m_B}{r_{AB}} \right] - \frac{20}{21} \frac{d}{dt} \left[m_A (x_A^i x_A^j x_A^k)^{\text{STF}} v_A^k \right] \right.$$

$$+ \frac{1}{14} \frac{d^2}{dt^2} \left[m_A x_A^2 (x_A^i x_A^j)^{\text{STF}} \right] + 4 \left[x_A^i (\mathbf{v}_A \times \mathbf{S}_A)^j \right]^{\text{STF}} - \frac{4}{3} \frac{d}{dt} \left[x_A^i (\mathbf{x}_A \times \mathbf{S}_A)^j \right]^{\text{STF}} \right\}. \tag{3.12}$$

We rewrite the mass quadrupole moment in relative coordinates by using the transformations

$$\mathbf{x}_1 = \mathbf{x} \left[\frac{m_2}{m} + \frac{1}{2} \eta \frac{\delta m}{m} \left(v^2 - \frac{m}{r} \right) \right] + \frac{\eta}{m} (\mathbf{v} \times \boldsymbol{\Delta}), \tag{3.13a}$$

$$\mathbf{x}_2 = \mathbf{x} \left[-\frac{m_1}{m} + \frac{1}{2} \eta \frac{\delta m}{m} \left(v^2 - \frac{m}{r} \right) \right] + \frac{\eta}{m} (\mathbf{v} \times \boldsymbol{\Delta}), \tag{3.13b}$$

which can be obtained from a constant of the motion that can be taken as the center of mass [28].

The relative mass quadrupole moment to (post)$^{3/2}$-Newtonian order is

$$I^{ij} = \mu \left(x^i x^j \right)^{\text{STF}} \left[1 + \frac{29}{42} (1 - 3\eta) v^2 - \frac{1}{7} (5 - 8\eta) \frac{m}{r} \right]$$

$$- \frac{4}{7} (1 - 3\eta) \mu r \dot{r} (x^i v^j)^{\text{STF}}$$

$$+ \frac{11}{21} (1 - 3\eta) \mu r^2 (v^i v^j)^{\text{STF}} + \frac{8}{3} \eta \left[x^i (\mathbf{v} \times \boldsymbol{\xi})^j \right]^{\text{STF}}$$

$$- \frac{4}{3} \eta \left[v^i (\mathbf{x} \times \boldsymbol{\xi})^j \right]^{\text{STF}} + I_{\text{tail}}^{ij}, \tag{3.14a}$$

where $\boldsymbol{\xi} \equiv \mathbf{S} + \frac{\delta m}{m} \boldsymbol{\Delta}$, and where I_{tail}^{ij} is a reminder that tail effects need to be included at (post)$^{3/2}$-Newtonian order. See Wiseman [6] and Blanchet and Damour [29] for more details on gravitational wave tails.

Note that the spin-orbit correction is a (post)$^{3/2}$-Newtonian correction for compact objects. Since a spin-orbit contribution to a multipole requires a term involving $\bar{v}_A$ and a spin-spin contribution $\bar{v}_A \bar{v}_B$, it is easy to see

that Eq. (3.2) implies that there are no spin-orbit corrections to the higher mass multipole moments at lowest order and no spin-spin contributions at lowest order or at post-Newtonian order. Therefore the remaining mass multipole moments to the appropriate order are as given by Wiseman [4]:

$$
I^{ijk} = -\mu \frac{\delta m}{m} \left\{ \left(x^i x^j x^k \right)^{\mathrm{STF}} \left[1 + \frac{1}{6}(5 - 19\eta)v^2 \right. \right.
$$
$$
\left. - \frac{1}{6}(5 - 13\eta)\frac{m}{r} \right] - (1 - 2\eta)r\dot{r}(x^i x^j v^k)^{\mathrm{STF}}
$$
$$
\left. + (1 - 2\eta)r^2(x^i v^j v^k)^{\mathrm{STF}} \right\}, \qquad (3.14b)
$$

$$
I^{ijkl} = \mu(1 - 3\eta) \left(x^i x^j x^k x^l \right)^{\mathrm{STF}}, \qquad (3.14c)
$$

$$
I^{ijklm} = -\mu \frac{\delta m}{m}(1 - 2\eta) \left(x^i x^j x^k x^l x^m \right)^{\mathrm{STF}}. \qquad (3.14d)
$$

2. Current multipole moments

The current multipole moments are given to lowest order as

$$
J^{iL} = \left\{ \epsilon^{iab} \int \sigma^b x^{aL} d^3x \right\}^{\mathrm{STF}}. \qquad (3.15)
$$

At leading order, the current quadrupole moment J^{ij} is a moment of angular momentum density; thus it will give an orbital angular momentum contribution as well as a spin contribution [effectively at $O(\epsilon^{1/2})$]. Although there is also a post-Newtonian correction to the current quadrupole moment, spin-orbit terms arising from this correction will be effectively a $(\mathrm{post})^{3/2}$-Newtonian correction, which is higher than we need, since the contribution of J^{ij} to the waveform is already $O(\epsilon^{1/2})$ at leading order.

Substituting Eqs. (3.3) and (3.4) into Eq. (3.15) we obtain

$$
J^{ij} = \left[\sum_A \epsilon^{iab} \int_A \rho^*(\mathbf{x}) v^b x^a x^j d^3x \right]^{\mathrm{STF}}, \qquad (3.16)
$$

for the current quadrupole moment.

Substituting $x^i = x_A^i + \bar{x}_A^i$ and $v^i = v_A^i + \bar{v}_A^i$ into Eq. (3.16), using the center-of-mass definition Eq. (3.6), and neglecting terms of $O(\beta^2)$, we obtain

$$
J^{ij} = \left\{ \sum_A \epsilon^{iab} \left[m_A x_A^a x_A^j v_A^b + x_A^a \int_A \rho^*(\mathbf{x}) \bar{x}_A^j \bar{v}_A^b d^3x \right. \right.
$$
$$
\left. \left. + x_A^j \int_A \rho^*(\mathbf{x}) \bar{x}_A^a \bar{v}_A^b d^3x \right] \right\}^{\mathrm{STF}}. \qquad (3.17)
$$

Using Eq. (3.10) the current quadrupole moment is then given by

$$
J^{ij} = \sum_A \left\{ m_A \left[x_A^i (\mathbf{x}_A \times \mathbf{v}_A)^j \right]^{\mathrm{STF}} + \frac{3}{2} \left(x_A^i S_A^j \right)^{\mathrm{STF}} \right\}. \qquad (3.18)
$$

Note that the spin-orbit correction is effectively $(\mathrm{post})^{1/2}$-Newtonian order. Repeating the calculation for the current octopole moment we obtain

$$
J^{ijk} = \sum_A \left\{ m_A \left[x_A^i x_A^j (\mathbf{x}_A \times \mathbf{v}_A)^k \right]^{\mathrm{STF}} \right.
$$
$$
\left. + 2 \left(x_A^i x_A^j S_A^k \right)^{\mathrm{STF}} \right\}. \qquad (3.19)
$$

Transforming Eqs. (3.18) and (3.19) into relative coordinates and adding the post-Newtonian correction to the current quadrupole moment derived by Wiseman [4], we obtain

$$
J^{ij} = -\mu \frac{\delta m}{m} \left\{ \left[x^i (\mathbf{x} \times \mathbf{v})^j \right]^{\mathrm{STF}} \left[1 + \frac{1}{28}(13 - 68\eta)v^2 \right. \right.
$$
$$
\left. + \frac{1}{14}(27 + 30\eta)\frac{m}{r} \right] + \frac{5}{28}(1 - 2\eta)r\dot{r}
$$
$$
\left. \times \left[v^i (\mathbf{x} \times \mathbf{v})^j \right]^{\mathrm{STF}} \right\} - \frac{3}{2}\eta(x^i \Delta^j)^{\mathrm{STF}}, \qquad (3.20a)
$$

$$
J^{ijk} = \mu(1 - 3\eta) \left[x^i x^j (\mathbf{x} \times \mathbf{v})^k \right]^{\mathrm{STF}} + 2\eta(x^i x^j \xi^k)^{\mathrm{STF}}. \qquad (3.20b)
$$

The final moment we need is given by

$$
J^{ijkl} = -\mu \frac{\delta m}{m}(1 - 2\eta) \left[x^i x^j x^k (\mathbf{x} \times \mathbf{v})^l \right]^{\mathrm{STF}}. \qquad (3.20c)
$$

Note that there are no spin-spin contributions to the current multipole moments at this order.

B. Gravitational waveform

Taking time derivatives of the radiative multipole moments (3.14) and (3.20), substituting the equations of motion (2.1) where appropriate, and substituting the results into Eq. (3.1), the gravitational waveform is given by

$$
h^{ij} = \frac{2\mu}{D} \left[Q^{ij} + P^{0.5}Q^{ij} + PQ^{ij} + PQ_{\mathrm{SO}}^{ij} + P^{1.5}Q^{ij} \right.
$$
$$
\left. + P^{1.5}Q_{\mathrm{SO}}^{ij} + P^{1.5}Q_{\mathrm{tail}}^{ij} + P^2 Q_{\mathrm{SS}}^{ij} \right]_{\mathrm{TT}}, \qquad (3.21)
$$

where

$$
Q^{ij} = 2 \left[v^i v^j - \frac{m}{r}n^i n^j \right], \qquad (3.22a)
$$

$$P^{0.5}Q^{ij} = \frac{\delta m}{m}\left\{3\frac{m}{r}\left[2n^{(i}v^{j)} - \dot{r}n^in^j\right](\hat{\mathbf{N}}\cdot\hat{\mathbf{n}}) + \left[\frac{m}{r}n^in^j - 2v^iv^j\right](\hat{\mathbf{N}}\cdot\mathbf{v})\right\}, \tag{3.22b}$$

$$PQ^{ij} = \frac{1}{3}(1-3\eta)\left\{4\frac{m}{r}\left[3\dot{r}n^in^j - 8n^{(i}v^{j)}\right](\hat{\mathbf{N}}\cdot\hat{\mathbf{n}})(\hat{\mathbf{N}}\cdot\mathbf{v}) + 2\left[3v^iv^j - \frac{m}{r}n^in^j\right](\hat{\mathbf{N}}\cdot\mathbf{v})^2\right.$$
$$\left. + \frac{m}{r}\left[\left(3v^2 - 15\dot{r}^2 + 7\frac{m}{r}\right)n^in^j + 30\dot{r}n^{(i}v^{j)} - 14v^iv^j\right](\hat{\mathbf{N}}\cdot\hat{\mathbf{n}})^2\right\} + \frac{4}{3}\frac{m}{r}\dot{r}(5+3\eta)n^{(i}v^{j)}$$
$$+ \left[(1-3\eta)v^2 - \frac{2}{3}(2-3\eta)\frac{m}{r}\right]v^iv^j + \frac{m}{r}\left[(1-3\eta)\dot{r}^2 - \frac{1}{3}(10+3\eta)v^2 + \frac{29}{3}\frac{m}{r}\right]n^in^j, \tag{3.22c}$$

$$PQ^{ij}_{\text{SO}} = \frac{2}{r^2}(\boldsymbol{\Delta}\times\hat{\mathbf{N}})^{(i}n^{j)}, \tag{3.22d}$$

$$P^{1.5}Q^{ij} = \frac{\delta m}{m}(1-2\eta)\left\{\frac{1}{4}\frac{m}{r}\left[(45\dot{r}^2 - 9v^2 - 28\frac{m}{r})n^in^j + 58v^iv^j - 108\dot{r}n^{(i}v^{j)}\right](\hat{\mathbf{N}}\cdot\hat{\mathbf{n}})^2(\hat{\mathbf{N}}\cdot\mathbf{v})\right.$$
$$+ \frac{1}{2}\left[\frac{m}{r}n^in^j - 4v^iv^j\right](\hat{\mathbf{N}}\cdot\mathbf{v})^3 + \frac{m}{r}\left[\frac{5}{4}(3v^2 - 7\dot{r}^2 + 6\frac{m}{r})\dot{r}n^in^j - \frac{1}{6}(21v^2 - 105\dot{r}^2\right.$$
$$\left. + 44\frac{m}{r})n^{(i}v^{j)} - \frac{17}{2}\dot{r}v^iv^j\right](\hat{\mathbf{N}}\cdot\hat{\mathbf{n}})^3 + \frac{3}{2}\frac{m}{r}\left[10n^{(i}v^{j)} - 3\dot{r}n^in^j\right](\hat{\mathbf{N}}\cdot\hat{\mathbf{n}})(\hat{\mathbf{N}}\cdot\mathbf{v})^2\right\}$$
$$+ \frac{\delta m}{m}\frac{1}{12}\frac{m}{r}(\hat{\mathbf{N}}\cdot\hat{\mathbf{n}})\left\{n^in^j\dot{r}\left[\dot{r}^2(15-90\eta) - v^2(63-54\eta) + \frac{m}{r}(242-24\eta)\right]\right.$$
$$\left. - \dot{r}v^iv^j(186+24\eta) + 2n^{(i}v^{j)}\left[\dot{r}^2(63+54\eta) - \frac{m}{r}(128-36\eta) + v^2(33-18\eta)\right]\right\}$$
$$+ \frac{\delta m}{m}(\hat{\mathbf{N}}\cdot\mathbf{v})\left\{\frac{1}{2}v^iv^j\left[\frac{m}{r}(3-8\eta) - 2v^2(1-5\eta)\right] - n^{(i}v^{j)}\frac{m}{r}\dot{r}(7+4\eta)\right.$$
$$\left. - n^in^j\frac{m}{r}\left[\frac{3}{4}(1-2\eta)\dot{r}^2 + \frac{1}{3}(26-3\eta)\frac{m}{r} - \frac{1}{4}(7-2\eta)v^2\right]\right\}, \tag{3.22e}$$

$$P^{1.5}Q^{ij}_{\text{SO}} = \frac{2}{r^2}\left\{n^in^j\left[(\hat{\mathbf{n}}\times\mathbf{v})\cdot\left(12\mathbf{S} + 6\frac{\delta m}{m}\boldsymbol{\Delta}\right)\right] - n^{(i}\left[\mathbf{v}\times\left(9\mathbf{S} + 5\frac{\delta m}{m}\boldsymbol{\Delta}\right)\right]^{j)}\right.$$
$$+ \left[3\dot{r}(\hat{\mathbf{N}}\cdot\hat{\mathbf{n}}) - 2(\hat{\mathbf{N}}\cdot\mathbf{v})\right]\left[\left(\mathbf{S} + \frac{\delta m}{m}\boldsymbol{\Delta}\right)\times\hat{\mathbf{N}}\right]^{(i}n^{j)} - v^{(i}\left[\hat{\mathbf{n}}\times\left(2\mathbf{S} + 2\frac{\delta m}{m}\boldsymbol{\Delta}\right)\right]^{j)}$$
$$+ \dot{r}n^{(i}\left[\hat{\mathbf{n}}\times\left(12\mathbf{S} + 6\frac{\delta m}{m}\boldsymbol{\Delta}\right)\right]^{j)} - 2(\hat{\mathbf{N}}\cdot\hat{\mathbf{n}})\left[\left(\mathbf{S} + \frac{\delta m}{m}\boldsymbol{\Delta}\right)\times\hat{\mathbf{N}}\right]^{(i}v^{j)}\right\}, \tag{3.22f}$$

$$P^{1.5}Q^{ij}_{\text{tail}} = 2\frac{m}{\mu}\int_0^\infty \overset{(4)}{I^{ij}_{\text{N}}}(u-u')\left[\ln\left(\frac{u'}{2s}\right) + \frac{11}{12}\right]du', \tag{3.22g}$$

$$P^2Q^{ij}_{\text{SS}} = -\frac{6}{\mu r^3}\left\{n^in^j\left[(\mathbf{S}_1\cdot\mathbf{S}_2) - 5(\hat{\mathbf{n}}\cdot\mathbf{S}_1)(\hat{\mathbf{n}}\cdot\mathbf{S}_2)\right] + 2n^{(i}S_1^{j)}(\hat{\mathbf{n}}\cdot\mathbf{S}_2) + 2n^{(i}S_2^{j)}(\hat{\mathbf{n}}\cdot\mathbf{S}_1)\right\}, \tag{3.22h}$$

where Q^{ij} is just the standard quadrupole term, $P^{0.5}Q^{ij}$ and PQ^{ij} were derived by Wagoner and Will [30], $P^{1.5}Q^{ij}$ was derived by Wiseman [4], and PQ^{ij}_{SO} and $P^{1.5}Q^{ij}_{\text{SO}}$ are the explicit spin-orbit corrections to the waveform. $P^{1.5}Q^{ij}_{\text{tail}}$ is the leading-order contribution to the waveform due to the tail, where $I^{ij}_{\text{N}} = \mu\left(x^ix^j\right)^{\text{STF}}$. Notice that it depends upon the past history of the binary's inspiral (u is a retarded time), and that s is an arbitrary matching parameter. See Wiseman [6] and Blanchet and Damour [29] for more details about gravita-

tional wave tails. Note that we have included the leading order spin-spin contribution to the waveform even though it is effectively a (post)^2-Newtonian term. It is due entirely to substituting $\mathbf{a}_{SS}$ into the time derivatives of the mass quadrupole moment. Note that we have simplified Eq. (3.21) by using relations such as

$$\left\{ \epsilon^{kl(i} \left[a^{j)} b^k \right]^{STF} N^l \right\}_{TT} = \left[\left(\mathbf{b} \times \hat{\mathbf{N}} \right)^{(i} a^{j)} \right]_{TT} .$$

Figure 4 shows the different contributions to the waveform for the final few orbits of an inspiraling binary system. We see that the spin-orbit contribution is comparable to the other post-Newtonian contributions, but the spin-spin contribution is almost negligible.

C. Energy loss

The radiative energy loss in terms of STF radiative multipoles is given by Thorne [22] as

$$\frac{dE}{dt} = -\frac{1}{5} \left\{ \overset{(3)}{I_{ij}} \overset{(3)}{I_{ij}} + \frac{5}{189} \overset{(4)}{I_{ijk}} \overset{(4)}{I_{ijk}} + \frac{16}{9} \overset{(3)}{J_{ij}} \overset{(3)}{J_{ij}} \right\}, \quad (3.23)$$

for the accuracy we require. Taking time derivatives of the radiative multipole moments (3.14) and (3.20), and substituting the equations of motion (2.1) where appropriate, the energy loss is given by

$$\frac{dE}{dt} = \dot{E}_N + \dot{E}_{PN} + \dot{E}_{SO} + \dot{E}_{tail} + \dot{E}_{SS}, \quad (3.24)$$

where

$$\dot{E}_N = -\frac{8}{15} \frac{m^2 \mu^2}{r^4} \left\{ 12v^2 - 11\dot{r}^2 \right\}, \quad (3.25a)$$

$$\dot{E}_{PN} = -\frac{2}{105} \frac{m^2 \mu^2}{r^4} \left\{ (785 - 852\eta)v^4 - 160(17 - \eta)\frac{m}{r}v^2 \right.$$
$$+ 8(367 - 15\eta)\frac{m}{r}\dot{r}^2 - 2(1487 - 1392\eta)v^2\dot{r}^2$$
$$\left. + 3(687 - 620\eta)\dot{r}^4 + 16(1 - 4\eta)\left(\frac{m}{r}\right)^2 \right\}, \quad (3.25b)$$

$$\dot{E}_{SO} = -\frac{8}{15} \frac{m\mu}{r^6} \left\{ \mathbf{L}_N \cdot \left[\mathbf{S}(78\dot{r}^2 - 80v^2 - 8\frac{m}{r}) \right. \right.$$
$$\left. \left. + \frac{\delta m}{m} \boldsymbol{\Delta}(51\dot{r}^2 - 43v^2 + 4\frac{m}{r}) \right] \right\}, \quad (3.25c)$$

$$\dot{E}_{tail} = -\frac{2}{5}\mu \overset{(3)}{I_N^{ij}} \frac{d}{du} P^{1.5} Q_{tail}^{ij}, \quad (3.25d)$$

$$\dot{E}_{SS} = -\frac{4}{15} \frac{m\mu}{r^6} \left\{ -3(\hat{\mathbf{n}} \cdot \mathbf{S}_1)(\hat{\mathbf{n}} \cdot \mathbf{S}_2)\left(168v^2 - 269\dot{r}^2\right) \right.$$
$$+ 3(\mathbf{S}_1 \cdot \mathbf{S}_2)\left(47v^2 - 55\dot{r}^2\right) + 71(\mathbf{v} \cdot \mathbf{S}_1)(\mathbf{v} \cdot \mathbf{S}_2)$$
$$\left. - 171\dot{r}\left[(\mathbf{v} \cdot \mathbf{S}_1)(\hat{\mathbf{n}} \cdot \mathbf{S}_2) + (\hat{\mathbf{n}} \cdot \mathbf{S}_1)(\mathbf{v} \cdot \mathbf{S}_2)\right] \right\}, \quad (3.25e)$$

where $\dot{E}_{PN}$ was found by Wagoner and Will [30] and $\dot{E}_{SO}$ and $\dot{E}_{SS}$ were reported in our previous paper [13]. $\dot{E}_{tail}$ depends upon the past history of the system and can only be evaluated explicitly for simple cases. Notice that the spin-spin contribution to the energy loss, which is effectively a (post)^2-Newtonian correction, comes from using post-Newtonian equations of motion in the derivatives of the mass quadrupole, and also from the contraction of the current quadrupoles. We have ignored (spin)^2-terms which are the same order as the spin-spin terms. In Fig. 7 we compare the spin contributions to the energy loss with the other contributions for an inspiraling binary system. Again we see that the spin-orbit contribution can be significant, while the spin-spin contribution is almost negligible.

D. Angular momentum loss

The radiative angular momentum loss in terms of STF radiative multipoles is given by Thorne [22] as

$$\frac{dJ^i}{dt} = -\frac{2}{5}\epsilon_{ijk} \left\{ \overset{(2)}{I_{jl}} \overset{(3)}{I_{kl}} + \frac{5}{126} \overset{(3)}{I_{jlm}} \overset{(4)}{I_{klm}} + \frac{16}{9} \overset{(2)}{J_{jl}} \overset{(3)}{J_{kl}} \right\},$$

$$(3.26)$$

for the accuracy we require. Taking time derivatives of the radiative multipole moments (3.14) and (3.20), and substituting the equations of motion (2.1) where appropriate, the angular momentum loss is given by

$$\frac{d\mathbf{J}}{dt} = \dot{\mathbf{J}}_N + \dot{\mathbf{J}}_{PN} + \dot{\mathbf{J}}_{SO} + \dot{\mathbf{J}}_{tail} + \dot{\mathbf{J}}_{SS}, \quad (3.27)$$
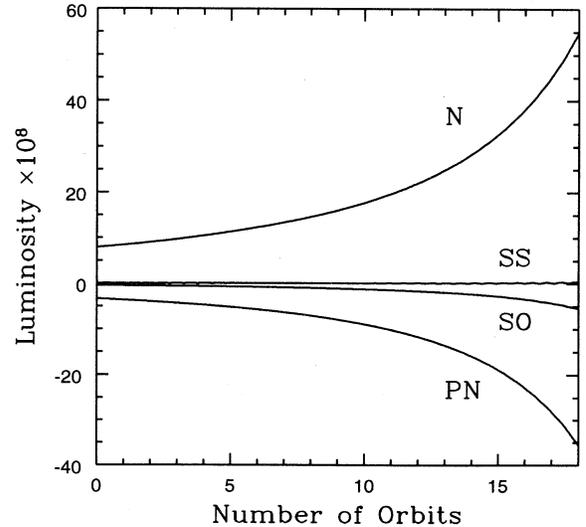
where

FIG. 7. The energy lost due to gravitational radiation plotted against orbital phase for a 10:1.4 mass-ratio system (with spins initially aligned as in Fig. 4). Plots begin at an orbital separation of $15m$ and terminate at $10m$. Plotted are the lowest-order Newtonian (N), post-Newtonian (PN), spin-orbit (SO), and spin-spin (SS) contributions to the energy loss.

$$\dot{\mathbf{J}}_{\mathrm{N}} = -\frac{8}{5}\frac{m\mu}{r^5}\mathbf{L}_{\mathrm{N}}\left\{2v^2 - 3\dot{r}^2 + 2\frac{m}{r}\right\}, \tag{3.28a}$$

$$\dot{\mathbf{J}}_{\mathrm{PN}} = -\frac{2}{105}\frac{m\mu}{r^5}\mathbf{L}_{\mathrm{N}}\left\{(307 - 548\eta)v^4 - 6(74 - 277\eta)v^2\dot{r}^2 + 2(372 + 197\eta)\frac{m}{r}\dot{r}^2\right.$$

$$\left. + 15(19 - 72\eta)\dot{r}^4 - 4(58 + 95\eta)\frac{m}{r}v^2 - 2(745 - 2\eta)\left(\frac{m}{r}\right)^2\right\}, \tag{3.28b}$$

$$\dot{\mathbf{J}}_{\mathrm{SO}} = -\frac{4}{5}\frac{\mu^2}{r^3}\left\{\frac{2}{3}\frac{m}{r}(\dot{r}^2 - v^2)\frac{\delta m}{m}\boldsymbol{\Delta} - \dot{r}\frac{m}{r}\hat{\mathbf{n}}\times\left[4(\mathbf{v}\times\mathbf{S}) + \frac{5}{3}\frac{\delta m}{m}(\mathbf{v}\times\boldsymbol{\Delta})\right]\right.$$

$$+ \frac{m}{r}\hat{\mathbf{n}}\times\left[(\hat{\mathbf{n}}\times\mathbf{S})\left(15\dot{r}^2 - \frac{41}{3}v^2 + \frac{4}{3}\frac{m}{r}\right) + \frac{\delta m}{m}(\hat{\mathbf{n}}\times\boldsymbol{\Delta})\left(9\dot{r}^2 - 8v^2 - \frac{2}{3}\frac{m}{r}\right)\right]$$

$$+ \dot{r}\mathbf{v}\times\left[(\hat{\mathbf{n}}\times\mathbf{S})\left(18\frac{m}{r} + 44v^2 - 55\dot{r}^2\right) + 5\frac{\delta m}{m}(\hat{\mathbf{n}}\times\boldsymbol{\Delta})\left(\frac{5}{3}\frac{m}{r} + 4v^2 - 5\dot{r}^2\right)\right]$$

$$+ \mathbf{v}\times\left[(\mathbf{v}\times\mathbf{S})\left(36\dot{r}^2 - \frac{71}{3}v^2 - \frac{50}{3}\frac{m}{r}\right) + \frac{\delta m}{m}(\mathbf{v}\times\boldsymbol{\Delta})\left(18\dot{r}^2 - \frac{35}{3}v^2 - 9\frac{m}{r}\right)\right]$$

$$\left. + \frac{\mathbf{L}_{\mathrm{N}}}{\mu^2 r^2}\mathbf{L}_{\mathrm{N}}\cdot\left[\left(65\dot{r}^2 - 37v^2 - \frac{163}{3}\frac{m}{r}\right)\mathbf{S} + \left(35\dot{r}^2 - 19v^2 - \frac{71}{3}\frac{m}{r}\right)\frac{\delta m}{m}\boldsymbol{\Delta}\right]\right\}, \tag{3.28c}$$

$$\dot{\mathbf{J}}_{\mathrm{tail}} = -\frac{2}{5}\mu\epsilon^{ijk}\left\{\overset{(3)}{I_{\mathrm{N}}^{kl}}\, P^{1.5}Q_{\mathrm{tail}}^{jl} + \overset{(2)}{I_{\mathrm{N}}^{jl}}\,\frac{d}{du}P^{1.5}Q_{\mathrm{tail}}^{kl}\right\}, \tag{3.28d}$$

$$\dot{\mathbf{J}}_{\mathrm{SS}} = -\frac{2}{5}\mu\epsilon^{ijk}\left\{\overset{(2)}{I_{\mathrm{N}}^{jl}}(\mathbf{a}_{\mathrm{N}})\,\overset{(3)}{I_{\mathrm{N}}^{kl}}(\mathbf{a}_{\mathrm{SS}}) + \overset{(2)}{I_{\mathrm{N}}^{jl}}(\mathbf{a}_{\mathrm{SS}})\,\overset{(3)}{I_{\mathrm{N}}^{kl}}(\mathbf{a}_{\mathrm{N}}) + \frac{16}{9}\overset{(2)}{J_{\mathrm{SO}}^{jl}}(\mathbf{a}_{\mathrm{N}})\,\overset{(3)}{J_{\mathrm{SO}}^{kl}}(\mathbf{a}_{\mathrm{N}})\right\}, \tag{3.28e}$$

where $\dot{\mathbf{J}}_{\mathrm{PN}}$ was calculated by Junker and Schäfer [31]. Note that $\dot{\mathbf{J}}_{\mathrm{tail}}$ depends upon the past history of the system. To avoid lengthy expressions, we have left $\dot{\mathbf{J}}_{\mathrm{SS}}$ in terms of derivatives of the multipole moments, where we have specified which contribution to the equations of motion should be substituted for the accelerations which appear in the time derivatives. Note that while $\dot{\mathbf{J}}_{\mathrm{N}}$ and $\dot{\mathbf{J}}_{\mathrm{PN}}$ are in the direction of $\mathbf{L}_{\mathrm{N}}$, in general $\dot{\mathbf{J}}_{\mathrm{SO}}$ and $\dot{\mathbf{J}}_{\mathrm{SS}}$ are not.

E. Linear momentum loss

The radiative linear momentum loss in terms of STF radiative multipoles is given by Thorne [22] as

$$\frac{dP^i}{dt} = -\left\{\frac{2}{63}\overset{(4)}{I_{ijk}}\overset{(3)}{I_{jk}} + \frac{16}{45}\epsilon_{ijk}\overset{(3)}{I_{jl}}\overset{(3)}{J_{kl}}\right\}, \tag{3.29}$$

for the accuracy we require. Taking time derivatives of the radiative multipole moments (3.14) and (3.20), and substituting the equations of motion (2.1) where appropriate, the linear momentum loss is given by

$$\frac{d\mathbf{P}}{dt} = \dot{\mathbf{P}}_{\mathrm{N}} + \dot{\mathbf{P}}_{\mathrm{SO}}, \tag{3.30}$$

where

$$\dot{\mathbf{P}}_{\mathrm{N}} = -\frac{8}{105}\frac{\delta m}{m}\eta^2\left(\frac{m}{r}\right)^4\left\{\dot{r}\hat{\mathbf{n}}\left[55v^2 - 45\dot{r}^2 + 12\frac{m}{r}\right]\right.$$

$$\left. + \mathbf{v}\left[38\dot{r}^2 - 50v^2 - 8\frac{m}{r}\right]\right\}, \tag{3.31a}$$

$$\dot{\mathbf{P}}_{\mathrm{SO}} = -\frac{8}{15}\frac{\mu^2 m}{r^5}\left\{4\dot{r}(\mathbf{v}\times\boldsymbol{\Delta}) - 2v^2(\hat{\mathbf{n}}\times\boldsymbol{\Delta})\right.$$

$$\left. - (\hat{\mathbf{n}}\times\mathbf{v})\left[3\dot{r}(\hat{\mathbf{n}}\cdot\boldsymbol{\Delta}) + 2(\mathbf{v}\cdot\boldsymbol{\Delta})\right]\right\}, \tag{3.31b}$$

where $\dot{\mathbf{P}}_{\mathrm{N}}$ was studied by Fitchett [32]. Note that $\dot{\mathbf{P}}_{\mathrm{SO}}$, which is effectively a $(\mathrm{post})^{1/2}$-Newtonian correction, can be directed out of the orbital plane. There is no spin-spin contribution to the linear momentum loss at this order. Wiseman [4] has derived the post-Newtonian corrections to $\dot{\mathbf{P}}$. In Fig. 8 we plot the momentum ejected for a typical inspiral. Notice that even in the presence of spinning bodies, the momentum ejection is periodic, and therefore there is no large buildup of momentum ejected in a specific direction.
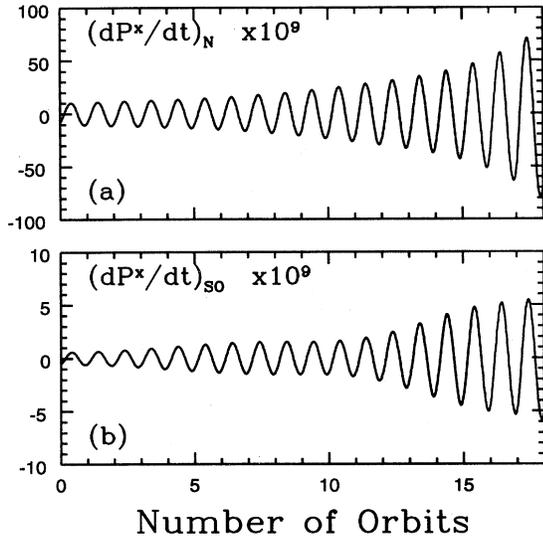
FIG. 8. The linear momentum ejected due to gravitational radiation plotted against orbital phase for a 10:1.4 mass-ratio system (with spins initially aligned as in Fig. 4). Plots begin at an orbital separation of $15m$ and terminate at $10m$.

IV. CIRCULAR ORBITS

A. Circular orbit limit

Gravitational radiation tends to circularize the orbit of an inspiraling binary. Therefore we would like to examine the last several minutes of the inspiral with the assumption that the orbit is quasicircular; that is, the orbit is circular on an orbital time scale, but inspirals on a radiation-reaction time scale. This is a reasonable assumption, since Lincoln and Will [3] have shown that virtually all captured binaries will have sufficient time to circularize their orbits before plunging to coalescence.

The equations of motion can be rewritten using the identities

$$\hat{\mathbf{n}} \cdot \mathbf{a} = \ddot{r} - r\omega^2, \tag{4.1a}$$

$$\hat{\lambda} \cdot \mathbf{a} = r\dot{\omega} + 2\dot{r}\omega, \tag{4.1b}$$

$$\hat{\mathbf{L}}_N \cdot \mathbf{a} = -r\omega \left(\hat{\lambda} \cdot \frac{d\hat{\mathbf{L}}_N}{dt} \right), \tag{4.1c}$$

where $\hat{\lambda} = \hat{\mathbf{L}}_N \times \hat{\mathbf{n}}$, $\hat{\mathbf{L}}_N = \mathbf{L}_N/|\mathbf{L}_N|$, and the orbital angular velocity ω is defined by $\mathbf{v} = \dot{r}\hat{\mathbf{n}} + r\omega\hat{\lambda}$. A circular orbit on a fixed plane is given by the solution $\ddot{r} = \dot{r} = \dot{\omega} = (d\hat{\mathbf{L}}_N/dt) = 0$. This solution exists if $r\omega^2 = -\hat{\mathbf{n}} \cdot \mathbf{a}$, $\hat{\lambda} \cdot \mathbf{a} = 0$, and $\hat{\mathbf{L}}_N \cdot \mathbf{a} = 0$, where we have substituted $\dot{r} = 0$ into the right-hand sides of Eqs. (4.1). Examining the equations of motion (2.1) (while ignoring the radiation-reaction terms), we see that circular orbit solutions exist only if the spins are aligned perpendicular to the orbital plane. If we instead define a circular orbit as one that has a constant orbital separation, but allow the orbital plane to precess, there exist circular orbit solutions for the case of one spinning body, but not for the case of both bodies spinning with general orientations.

If we first average the spin-orbit and spin-spin terms in the acceleration over an orbit, then we can obtain orbits of constant separation for arbitrary spins and orientations. In order to average over an orbit we need to assume that the spins and orbital plane remain constant over an orbital period, in other words, that ω_p/ω is small. For circular orbits

$$m\omega = \left(\frac{m}{r}\right)^{3/2}, \tag{4.2}$$

to leading order. Using Eq. (2.14) for the case of one spinning body we see that

$$\frac{\omega_p}{\omega} = \frac{1}{2}\frac{|\mathbf{J}|}{m^2}\left(\frac{m}{r}\right)^{3/2}\left[1 + 3\frac{m}{m_s}\right]. \tag{4.3}$$

Since $|\mathbf{J}| \leq |\mathbf{L}| + |\mathbf{S}|$, $|\mathbf{L}|/m^2 = \eta(r/m)^{1/2}$, and $|\mathbf{S}|/m^2 = \chi(m_s/m)^2$, where $\chi \leq 1$, then we see that

$$\frac{\omega_p}{\omega} \leq \frac{1}{2}\left\{ \left(\frac{m}{r}\right)\left[\eta + 3\frac{m - m_s}{m}\right] + \chi\left(\frac{m}{r}\right)^{3/2}\frac{m_s}{m}\left[3 + \frac{m_s}{m}\right] \right\}, \tag{4.4}$$

which is small $[= O(m/r)]$ until the very late stages of the inspiral, where the whole circular orbit approximation breaks down anyway. We would expect a similar argument to hold for the case where both bodies are spinning, since the spins' instantaneous precessions have a form similar to that of the precession in the single spin case (see Sec. II B). An examination of numerical evolutions of the precession equations confirms this.

In examining circular orbits, we will assume an orbit where $\dot{r} = 0$ and $r\omega^2 = -\langle\hat{\mathbf{n}} \cdot \mathbf{a}\rangle$ where the brackets denote an average over an orbit. We therefore obtain the following expressions for a circular orbit. The orbital velocity is given by $v = r\omega$ where

$$r^2\omega^2 = \left(\frac{m}{r}\right)\left\{ 1 - (3 - \eta)\left(\frac{m}{r}\right) - \sum_{i=1,2}\left[\chi_i(\hat{\mathbf{L}}_N \cdot \hat{\mathbf{s}}_i)\left(2\frac{m_i^2}{m^2} + 3\eta\right)\right]\left(\frac{m}{r}\right)^{3/2} + \left[\left(6 + \frac{41}{4}\eta + \eta^2\right) - \frac{3}{2}\eta\chi_1\chi_2\left[(\hat{\mathbf{s}}_1 \cdot \hat{\mathbf{s}}_2) - 3(\hat{\mathbf{L}}_N \cdot \hat{\mathbf{s}}_1)(\hat{\mathbf{L}}_N \cdot \hat{\mathbf{s}}_2)\right]\right]\left(\frac{m}{r}\right)^2 \right\}, \tag{4.5}$$

where $\mathbf{S}_A = \chi_A m_A^2 \hat{\mathbf{s}}_A$. The energy and angular momentum are given by

$$E = -\frac{1}{2}\frac{\mu m}{r}\left\{1 - \frac{1}{4}(7-\eta)\left(\frac{m}{r}\right) + \sum_{i=1,2}\left[\chi_i(\hat{\mathbf{L}}_N \cdot \hat{s}_i)\left(2\frac{m_i^2}{m^2} + \eta\right)\right]\left(\frac{m}{r}\right)^{3/2}\right.$$

$$\left. - \left[\frac{1}{8}(7 - 49\eta - \eta^2) - \frac{1}{2}\eta\chi_1\chi_2\left[(\hat{\mathbf{s}}_1 \cdot \hat{\mathbf{s}}_2) - 3(\hat{\mathbf{L}}_N \cdot \hat{\mathbf{s}}_1)(\hat{\mathbf{L}}_N \cdot \hat{\mathbf{s}}_2)\right]\right]\left(\frac{m}{r}\right)^2\right\}, \tag{4.6}$$

$$\mathbf{J} = \mu(mr)^{1/2}\hat{\mathbf{L}}_N\left\{1 + 2\left(\frac{m}{r}\right) - \frac{1}{4}\sum_{i=1,2}\left[\chi_i(\hat{\mathbf{L}}_N \cdot \hat{s}_i)\left(8\frac{m_i^2}{m^2} + 7\eta\right)\right]\left(\frac{m}{r}\right)^{3/2} + \left[\frac{1}{2}(5 - 9\eta)\right.\right.$$

$$\left.\left. - \frac{3}{4}\eta\chi_1\chi_2\left[(\hat{\mathbf{s}}_1 \cdot \hat{\mathbf{s}}_2) - 3(\hat{\mathbf{L}}_N \cdot \hat{\mathbf{s}}_1)(\hat{\mathbf{L}}_N \cdot \hat{\mathbf{s}}_2)\right]\right]\left(\frac{m}{r}\right)^2\right\} + \mathbf{S} - \frac{1}{4}\mu(mr)^{1/2}\sum_{i=1,2}\left[\chi_i\hat{s}_i\left(4\frac{m_i^2}{m^2} + \eta\right)\right]\left(\frac{m}{r}\right)^{3/2}. \tag{4.7}$$

For a circular orbit, the waveform is given by

$$h^{ij} = \frac{2\mu}{D}\left(\frac{m}{r}\right)\left\{Q_c^{ij} + P^{0.5}Q_c^{ij}\left(\frac{m}{r}\right)^{1/2} + PQ_c^{ij}\left(\frac{m}{r}\right) + P^{1.5}Q_c^{ij}\left(\frac{m}{r}\right)^{3/2}\right\}_{TT}, \tag{4.8}$$

where

$$Q_c^{ij} = 2\left[\lambda^i\lambda^j - n^i n^j\right], \tag{4.9a}$$

$$P^{0.5}Q_c^{ij} = \frac{\delta m}{m}\left\{6(\hat{\mathbf{N}} \cdot \hat{\mathbf{n}})n^{(i}\lambda^{j)} + (\hat{\mathbf{N}} \cdot \hat{\lambda})\left[n^i n^j - 2\lambda^i\lambda^j\right]\right\}, \tag{4.9b}$$

$$PQ_c^{ij} = \frac{2}{3}(1 - 3\eta)\left\{(\hat{\mathbf{N}} \cdot \hat{\mathbf{n}})^2\left[5n^i n^j - 7\lambda^i\lambda^j\right] - 16(\hat{\mathbf{N}} \cdot \hat{\mathbf{n}})(\hat{\mathbf{N}} \cdot \hat{\lambda})n^{(i}\lambda^{j)}\right.$$

$$\left. + (\hat{\mathbf{N}} \cdot \hat{\lambda})^2\left[3\lambda^i\lambda^j - n^i n^j\right]\right\} + \frac{1}{3}(19 - 3\eta)(n^i n^j - \lambda^i\lambda^j) + \frac{2}{m^2}n^{(i}(\mathbf{\Delta} \times \hat{\mathbf{N}})^{j)}, \tag{4.9c}$$

$$P^{1.5}Q_c^{ij} = \frac{\delta m}{m}\left\{(1 - 2\eta)\left[\frac{1}{2}(\hat{\mathbf{N}} \cdot \hat{\lambda})^3\left(n^i n^j - 4\lambda^i\lambda^j\right) + \frac{1}{4}(\hat{\mathbf{N}} \cdot \hat{\mathbf{n}})^2(\hat{\mathbf{N}} \cdot \hat{\lambda})\left(58\lambda^i\lambda^j - 37n^i n^j\right)\right.\right.$$

$$\left. - \frac{65}{6}(\hat{\mathbf{N}} \cdot \hat{\mathbf{n}})^3 n^{(i}\lambda^{j)} + 15(\hat{\mathbf{N}} \cdot \hat{\mathbf{n}})(\hat{\mathbf{N}} \cdot \hat{\lambda})^2 n^{(i}\lambda^{j)}\right] - (\hat{\mathbf{N}} \cdot \hat{\lambda})\left[\frac{1}{12}(101 - 12\eta)n^i n^j\right.$$

$$\left. - \frac{1}{2}(19 - 4\eta)\lambda^i\lambda^j\right] - \frac{1}{6}(149 - 6\eta)(\hat{\mathbf{N}} \cdot \hat{\mathbf{n}})n^{(i}\lambda^{j)}\right\} - \frac{2}{m^2}\left\{\lambda^i\lambda^j\left[\hat{\mathbf{L}}_N \cdot \left(5\mathbf{S} + 3\frac{\delta m}{m}\mathbf{\Delta}\right)\right]\right.$$

$$\left. - 6n^i n^j\left[\hat{\mathbf{L}}_N \cdot \left(2\mathbf{S} + \frac{\delta m}{m}\mathbf{\Delta}\right)\right] + 2\lambda^{(i}\left[\hat{\mathbf{n}} \times \left(\mathbf{S} + \frac{\delta m}{m}\mathbf{\Delta}\right)\right]^{j)} + n^{(i}\left[\hat{\lambda} \times \left(9\mathbf{S} + 5\frac{\delta m}{m}\mathbf{\Delta}\right)\right]^{j)}\right.$$

$$\left. + 2\left(\hat{\mathbf{N}} \cdot \hat{\lambda}\right)\left[\left(\mathbf{S} + \frac{\delta m}{m}\mathbf{\Delta}\right) \times \hat{\mathbf{N}}\right]^{(i} n^{j)} + 2\left(\hat{\mathbf{N}} \cdot \hat{\mathbf{n}}\right)\left[\left(\mathbf{S} + \frac{\delta m}{m}\mathbf{\Delta}\right) \times \hat{\mathbf{N}}\right]^{(i}\lambda^{j)}\right\}, \tag{4.9d}$$

where $\lambda^i = v^i/|\mathbf{v}|$ for a circular orbit. The energy loss and angular momentum loss for a circular orbit are given by

$$\frac{dE}{dt} = -\frac{32}{5}\eta^2\left(\frac{m}{r}\right)^5\left(1 - \frac{1}{336}(2927 + 420\eta)\left(\frac{m}{r}\right) - \left\{\frac{1}{12}\sum_{i=1,2}\left[\chi_i(\hat{\mathbf{L}}_N \cdot \hat{s}_i)\left(73\frac{m_i^2}{m^2} + 75\eta\right)\right]\right.\right.$$

$$\left.\left. - 4\pi\right\}\left(\frac{m}{r}\right)^{3/2} - \frac{1}{48}\eta\chi_1\chi_2\left[223(\hat{\mathbf{s}}_1 \cdot \hat{\mathbf{s}}_2) - 649(\hat{\mathbf{L}}_N \cdot \hat{\mathbf{s}}_1)(\hat{\mathbf{L}}_N \cdot \hat{\mathbf{s}}_2)\right]\left(\frac{m}{r}\right)^2\right), \tag{4.10}$$

$$\frac{d\mathbf{J}}{dt} = -\frac{32}{5}\eta^2\left(\frac{m}{r}\right)^4(mr)^{1/2}\left[\hat{\mathbf{L}}_N\left(1 - \frac{1}{336}(2423 + 588\eta)\left(\frac{m}{r}\right) - \left\{\frac{1}{8}\sum_{i=1,2}\left[\chi_i(\hat{\mathbf{L}}_N \cdot \hat{s}_i)\left(53\frac{m_i^2}{m^2}\right.\right.\right.\right.$$

$$\left.\left.\left.\left. + 52\eta\right)\right]\right\} - 4\pi\right\}\left(\frac{m}{r}\right)^{3/2}\right) + \frac{1}{24}\sum_{i=1,2}\left[\chi_i\hat{s}_i\left(37\frac{m_i^2}{m^2} + 42\eta\right)\right]\left(\frac{m}{r}\right)^{3/2}\right], \tag{4.11}$$

where the 4π terms are due to the gravitational wave tail.

The rate of inspiral is given by $\dot{r} = (dE/dt)/(dE/dr)$. Taking Eq. (4.10) and dividing it by the derivative of Eq. (4.6), we obtain

$$
\frac{dr}{dt} = -\frac{64}{5}\eta\left(\frac{m}{r}\right)^3\left(1 - \frac{1}{336}(1751 + 588\eta)\left(\frac{m}{r}\right) - \left\{\frac{7}{12}\sum_{i=1,2}\left[\chi_i(\hat{\mathbf{L}}_N \cdot \hat{\mathbf{s}}_i)\left(19\frac{m_i^2}{m^2} + 15\eta\right)\right]\right.
$$

$$
\left. - 4\pi\right\}\left(\frac{m}{r}\right)^{3/2} - \frac{5}{48}\eta\chi_1\chi_2\left[59(\hat{\mathbf{s}}_1 \cdot \hat{\mathbf{s}}_2) - 173(\hat{\mathbf{L}}_N \cdot \hat{\mathbf{s}}_1)(\hat{\mathbf{L}}_N \cdot \hat{\mathbf{s}}_2)\right]\left(\frac{m}{r}\right)^2\right). \tag{4.12}
$$

The above expressions can be inverted to express everything in terms of the orbital frequency. For a given orbital frequency, the separation is given by

$$
(r/m) = (m\omega)^{-2/3}\left\{1 - \frac{1}{3}(3 - \eta)(m\omega)^{2/3} - \frac{1}{3}\sum_{i=1,2}\left[\chi_i(\hat{\mathbf{L}}_N \cdot \hat{\mathbf{s}}_i)\left(2\frac{m_i^2}{m^2} + 3\eta\right)\right](m\omega)\right.
$$

$$
\left. + \left[\eta\left(\frac{19}{4} + \frac{1}{9}\eta\right) - \frac{1}{2}\eta\chi_1\chi_2\left[(\hat{\mathbf{s}}_1 \cdot \hat{\mathbf{s}}_2) - 3(\hat{\mathbf{L}}_N \cdot \hat{\mathbf{s}}_1)(\hat{\mathbf{L}}_N \cdot \hat{\mathbf{s}}_2)\right]\right](m\omega)^{4/3}\right\}. \tag{4.13}
$$

Using Eqs. (4.12) and (4.13), we find that the evolution of the orbital frequency is given by

$$
\frac{\dot{\omega}}{\omega^2} = \frac{96}{5}\eta(m\omega)^{5/3}\left(1 - \frac{1}{336}(743 + 924\eta)(m\omega)^{2/3} - \left\{\frac{1}{12}\sum_{i=1,2}\left[\chi_i(\hat{\mathbf{L}}_N \cdot \hat{\mathbf{s}}_i)\left(113\frac{m_i^2}{m^2} + 75\eta\right)\right]\right.
$$

$$
\left. - 4\pi\right\}(m\omega) - \frac{1}{48}\eta\chi_1\chi_2\left[247(\hat{\mathbf{s}}_1 \cdot \hat{\mathbf{s}}_2) - 721(\hat{\mathbf{L}}_N \cdot \hat{\mathbf{s}}_1)(\hat{\mathbf{L}}_N \cdot \hat{\mathbf{s}}_2)\right](m\omega)^{4/3}\right). \tag{4.14}
$$

The evolution of the orbital frequency can be used to calculate the accumulated orbital phase of the binary. The orbital phase as observed by a phase sensitive detector such as LIGO or VIRGO is given by

$$
\Psi \equiv \int_{t_i}^{t_f} \omega\,dt = \int_{\omega_i}^{\omega_f} \frac{\omega}{\dot{\omega}}\,d\omega, \tag{4.15}
$$

where t_i is the time at which the signal enters the sensitive bandwidth (corresponding to a lower frequency ω_i set by seismic noise) and t_f is the time at which the signal leaves the sensitive bandwidth (corresponding to an upper frequency ω_f set by photon shot noise), the time at which the orbit begins to plunge (corresponding to a frequency ω_f of the innermost stable circular orbit), or the time when the two bodies begin to coalesce. The result is

$$
\Psi = \frac{1}{32\eta}\left\{\left[(m\omega_i)^{-5/3} - (m\omega_f)^{-5/3}\right] + \frac{5}{1008}(743 + 924\eta)\left[(m\omega_i)^{-1} - (m\omega_f)^{-1}\right]\right.
$$

$$
+ \left[\frac{5}{24}\sum_{i=1,2}\left[\chi_i(\hat{\mathbf{L}}_N \cdot \hat{\mathbf{s}}_i)\left(113\frac{m_i^2}{m^2} + 75\eta\right)\right] - 10\pi\right]\left[(m\omega_i)^{-2/3} - (m\omega_f)^{-2/3}\right]
$$

$$
\left. + \frac{5}{48}\eta\chi_1\chi_2\left[247(\hat{\mathbf{s}}_1 \cdot \hat{\mathbf{s}}_2) - 721(\hat{\mathbf{L}}_N \cdot \hat{\mathbf{s}}_1)(\hat{\mathbf{L}}_N \cdot \hat{\mathbf{s}}_2)\right]\left[(m\omega_i)^{-1/3} - (m\omega_f)^{-1/3}\right]\right\}. \tag{4.16}
$$

The term with 10π is the tail contribution to the orbital phase. Table I shows the contribution of each term to the orbital phase for several cases.

B. Radiation-reaction effects on the precessions

When averaged over a circular orbit, the orbital angular momentum and spins precess as

$$
\dot{\mathbf{L}} = \frac{1}{2r^3}\left\{\left[\left(4 + 3\frac{m_2}{m_1}\right)\mathbf{S}_1 + \left(4 + 3\frac{m_1}{m_2}\right)\mathbf{S}_2\right] \times \mathbf{L}_N\right.
$$

$$
\left. -3(\hat{\mathbf{L}}_N \cdot \mathbf{S}_2)\mathbf{S}_1 \times \hat{\mathbf{L}}_N - 3(\hat{\mathbf{L}}_N \cdot \mathbf{S}_1)\mathbf{S}_2 \times \hat{\mathbf{L}}_N\right\}, \tag{4.17a}
$$

$$
\dot{\mathbf{S}}_1 = \frac{1}{2r^3}\left\{(\mathbf{L}_N \times \mathbf{S}_1)\left(4 + 3\frac{m_2}{m_1}\right) + \mathbf{S}_2 \times \mathbf{S}_1\right.
$$

$$
\left. -3(\hat{\mathbf{L}}_N \cdot \mathbf{S}_2)\hat{\mathbf{L}}_N \times \mathbf{S}_1\right\}, \tag{4.17b}
$$

$$
\dot{\mathbf{S}}_2 = \frac{1}{2r^3}\left\{(\mathbf{L}_N \times \mathbf{S}_2)(4 + 3\frac{m_1}{m_2}) + \mathbf{S}_1 \times \mathbf{S}_2\right.
$$

$$
\left. -3(\hat{\mathbf{L}}_N \cdot \mathbf{S}_1)\hat{\mathbf{L}}_N \times \mathbf{S}_2\right\}. \tag{4.17c}
$$

Since $\langle \dot{\mathbf{L}}_{SO} \rangle = 0$ over an orbit, the precession of $\mathbf{L}_N$ is also given by Eq. (4.17a) with $\mathbf{L}$ replaced by $\mathbf{L}_N$. Thus we see that for a circular orbit the magnitudes of the vectors $\mathbf{L}$, $\mathbf{L}_N$, and $\mathbf{S}_i$ are conserved on average during precession in the absence of radiation reaction.

For a binary system inspiraling due to gravitational radiation, there is a loss of total angular momentum given by $\dot{\mathbf{J}}$. We assume that the individual spinning bodies are sufficiently axisymmetric that they will emit negligible gravitational radiation on their own, so that their spins are unaffected by radiation damping to the order which we are considering. (See Ref. [19] for a more rigorous argument.) This means that the angular momentum loss is entirely from the orbital angular momentum, and that the total change in orbital angular momentum is the sum of the precession and the radiation damping.

Let us examine this in more detail for the case of one spinning body, where we only consider the leading order damping effects. Then we have [see Eqs. (2.12)–(2.14)]

$$\dot{\mathbf{S}} = \omega_p \hat{\mathbf{J}} \times \mathbf{S}, \tag{4.18a}$$

$$\dot{\mathbf{L}}_N = \omega_p \hat{\mathbf{J}} \times \mathbf{L}_N - \epsilon_{RR} \mathbf{L}_N, \tag{4.18b}$$

$$\dot{\mathbf{J}} = -\epsilon_{RR} \mathbf{L}_N, \tag{4.18c}$$

where $\hat{\mathbf{J}} = \mathbf{J}/|\mathbf{J}|$, and where $\epsilon_{RR} = (32/5)(\mu/m^2)(m/r)^4$ is the rate of angular momentum loss due to gravitational radiation. Defining $L = |\mathbf{L}_N|$, $S = |\mathbf{S}|$, and $\kappa = \arccos\left(\hat{\mathbf{L}}_N \cdot \hat{\mathbf{S}}\right)$,

$$J = |\mathbf{J}| = \left\{ L^2 + S^2 + 2LS\cos\kappa \right\}^{1/2}, \tag{4.19a}$$

$$i = \cos^{-1}\left(\hat{\mathbf{L}}_N \cdot \hat{\mathbf{J}}\right) = \cos^{-1}\left\{ [L + S\cos\kappa]/J \right\}, \tag{4.19b}$$

we see that Eqs. (4.18) imply that

$$\dot{S} = 0, \tag{4.20a}$$

$$\dot{L} = -\epsilon_{RR} L, \tag{4.20b}$$

$$\dot{J} = -\epsilon_{RR} L \cos i, \tag{4.20c}$$

$$\dot{\kappa} = 0, \tag{4.20d}$$

$$\frac{di}{dt} = \frac{\epsilon_{RR} L}{J} \sin i. \tag{4.20e}$$

As the binary inspirals, $\mathbf{L}_N$ and $\mathbf{J}$ shrink and the angle between them grows. This is shown in Fig. 9. The angle κ between $\mathbf{L}_N$ and $\mathbf{S}$ remains fixed as they precess about $\mathbf{J}$, so that $\mathbf{S}$ tips toward $\mathbf{J}$ and at late times when $\mathbf{J} \approx \mathbf{S}$, i approaches κ. Working to first order in $(L\epsilon_{RR})/(J\omega_p)$, we can show that, if $\mathbf{J}_0$ is the initial direction of $\mathbf{J}$,
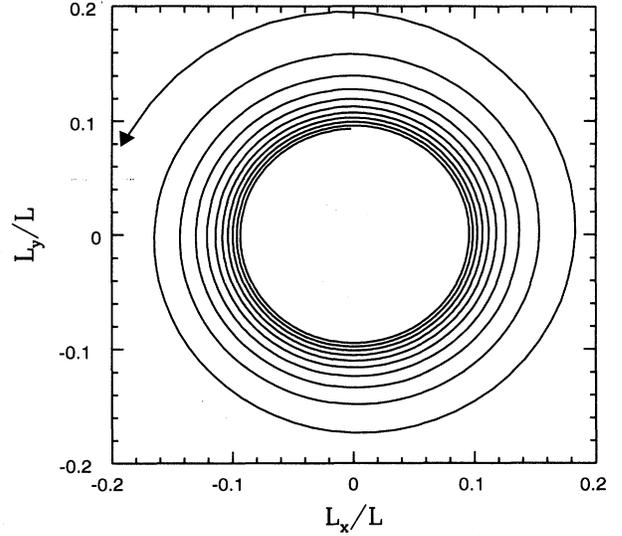

FIG. 9. The simple precession of the orbital angular momentum $\mathbf{L}$ in the presence of gravitational radiation damping for an inspiraling system with a 2:1 mass-ratio with only the larger body spinning (the spin is perpendicular to $\mathbf{L}$). Notice that the inclination of the orbital plane with respect to $\mathbf{J}_0$ increases as the binary inspirals ($i = \arcsin[(\hat{L}_x^2 + \hat{L}_y^2)^{1/2}]$).

$$\mathbf{J} = \frac{\epsilon_{RR}}{\omega_p} \left(\hat{\mathbf{J}}_0 \times \mathbf{L}_N \right) + \left[1 - \frac{\epsilon_{RR} L}{J}(t - t_0)\cos i \right] \hat{\mathbf{J}}_0 , \tag{4.21}$$

valid for $(t - t_0) << J/(L\epsilon_{RR})$, which implies that $\mathbf{J}$ spirals about $\mathbf{J}_0$ as it shrinks. As long as the ratio $\Lambda \equiv (L\epsilon_{RR})/(J\omega_p) \ll 1$, then $\hat{\mathbf{J}}$ will remain relatively fixed in space, precessing on a tight spiral around its earlier direction. If the ratio Λ is not small, however, $\mathbf{L}_N$ and $\mathbf{S}$ will still precess about $\mathbf{J}$, but $\mathbf{J}$ will start to tumble. An example of this would be if $\mathbf{L}$ and $\mathbf{S}$ were nearly equal in magnitude, but pointing in opposite directions so that $J = |\mathbf{L} + \mathbf{S}| \ll L$. This is the case of "transitional precession" described in Ref. [19].

If both bodies are spinning, the precessions of $\mathbf{L}$ and $\mathbf{S}$ are more complicated (as in Sec. II), but the effects of radiation damping are qualitatively the same. As the binary inspirals, $\mathbf{L}_N$ and $\mathbf{J}$ shrink and the maximum angle between them grows. $\mathbf{J}$ remains relatively fixed in direction as long as the precession time scale is shorter than the inspiral time scale, and as long as the ratio Λ is small, where we replace the precession frequency ω_p with the instantaneous precession frequencies $\omega_p^{(A)}$. Figure 10 shows an example of this. Numerical evolutions of the precession equations in the presence of radiation-reaction agree with our description above.

C. Wave polarization states

The gravitational radiation emitted by the binary can be written in terms of its two polarization states h_+ and $h_\times$. The polarization states can be expressed as linear
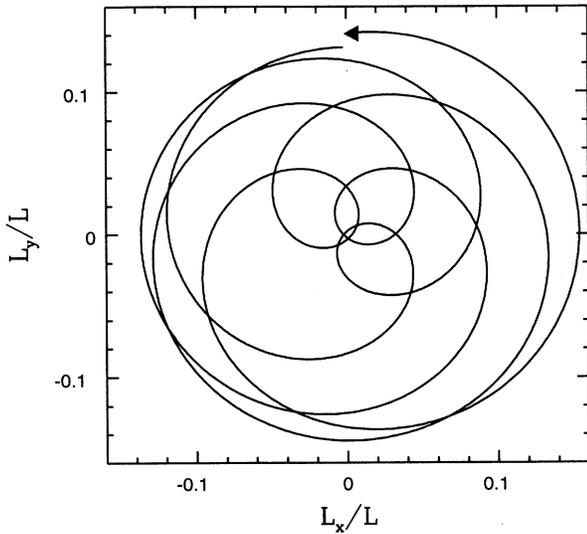
FIG. 10. The complicated precession of the orbital angular momentum **L** in the presence of gravitational radiation damping for an inspiraling system with a 2:1 mass-ratio and equal spins which are initially aligned, and perpendicular to **L**. Notice that the maximum inclination of the orbital plane increases as the binary inspirals.

combinations of the components of h^{ij} in some suitable coordinate system. Normally one chooses a coordinate system such that the orbital plane lies in the x-y plane, and the source and detector are located in the x-z plane as this simplifies the equations involved (see Ref. [33]). If the bodies are spinning, however, this coordinate system is not fixed in space. This does not prevent one from using such a coordinate system (see Apostolatos *et al.* [19]), but one must remember that it is precessing. Instead, we choose our coordinate system such that our z axis lies along some initial direction of **J**. We define $\Theta = \arccos\left(\hat{\mathbf{N}} \cdot \hat{\mathbf{J}}_0\right)$ and choose a coordinate system in which $\hat{\mathbf{z}} = \hat{\mathbf{J}}_0$ and $\hat{\mathbf{N}} = \cos\Theta\hat{\mathbf{z}} + \sin\Theta\hat{\mathbf{x}}$ lies in the x-z plane (see Fig. 2). (Note that if $\Theta = 0$, $\hat{\mathbf{x}}$ can be chosen arbitrarily.) Following the method of Finn and Chernoff [33] we define the radiation coordinate system such that

$$\mathbf{e}_z^R = \hat{\mathbf{N}}, \qquad (4.22a)$$

$$\mathbf{e}_y^R = \hat{\mathbf{y}} = \frac{\hat{\mathbf{J}}_0 \times \hat{\mathbf{N}}}{\left\{1 - (\hat{\mathbf{J}}_0 \cdot \hat{\mathbf{N}})^2\right\}^{1/2}}, \qquad (4.22b)$$

$$\mathbf{e}_x^R = \hat{\mathbf{y}} \times \hat{\mathbf{N}} = \frac{(\hat{\mathbf{J}}_0 \cdot \hat{\mathbf{N}})\hat{\mathbf{N}} - \hat{\mathbf{J}}_0}{\left\{1 - (\hat{\mathbf{J}}_0 \cdot \hat{\mathbf{N}})^2\right\}^{1/2}}. \qquad (4.22c)$$

Then from Eqs. (3.2) and (3.3) of Ref. [33], the radiation can be written in terms of its polarization states

$$h_+ = \tfrac{1}{2}\left\{\cos^2\Theta h^{xx} - h^{yy} + \sin^2\Theta h^{zz} - \sin 2\Theta h^{xz}\right\}, \qquad (4.23a)$$

$$h_\times = \cos\Theta h^{xy} - \sin\Theta h^{yz}. \qquad (4.23b)$$

The response of a detector will be the linear combination

$$h = F_+ h_+ + F_\times h_\times, \qquad (4.24)$$

where F_+ and $F_\times$ are the antenna patterns which depend upon the orientation of the detector with respect to the binary:

$$F_+ = \tfrac{1}{2}(1 + \cos^2\theta)\cos 2\phi \cos 2\psi - \cos\theta \sin 2\phi \sin 2\psi, \qquad (4.25a)$$

$$F_\times = \tfrac{1}{2}(1 + \cos^2\theta)\cos 2\phi \sin 2\psi + \cos\theta \sin 2\phi \cos 2\psi, \qquad (4.25b)$$

where (θ, ϕ) is the location of the binary with respect to the detector (whose arms lie along the $\bar{x}$ and $\bar{y}$ axes in the detector's coordinate system, with the $\bar{z}$ axis in the vertical direction), and ψ is the polarization angle between the gravitational waves' polarization axes and the direction of constant azimuth. (See Fig. 11.) For our definition of the polarization axes, the polarization angle is given by

$$\psi = \arctan\left(\frac{\hat{\mathbf{N}} \cdot (\hat{\mathbf{J}}_0 \times \hat{\bar{\mathbf{z}}})}{\hat{\mathbf{J}}_0 \cdot \hat{\bar{\mathbf{z}}} - (\hat{\mathbf{J}}_0 \cdot \hat{\mathbf{N}})(\hat{\bar{\mathbf{z}}} \cdot \hat{\mathbf{N}})}\right). \qquad (4.26)$$

If $\hat{\mathbf{N}} = \pm\hat{\bar{\mathbf{z}}}$, then

$$\psi = \arctan\left[-(\hat{\mathbf{N}} \cdot \hat{\bar{\mathbf{z}}})\frac{\hat{\bar{\mathbf{y}}} \cdot \hat{\mathbf{J}}_0}{\hat{\bar{\mathbf{x}}} \cdot \hat{\mathbf{J}}_0}\right]. \qquad (4.27)$$
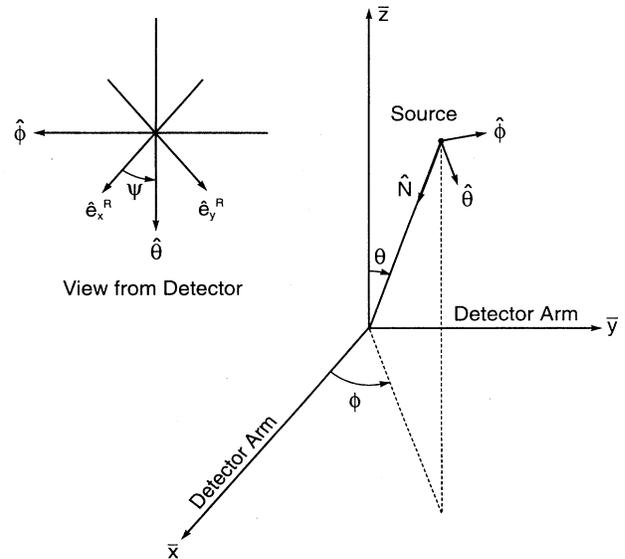

FIG. 11. The detector coordinate system. The detectors arms lie along the $\bar{x}$ and $\bar{y}$ axes. The angles (θ, ϕ) define the location of the source, and the polarization angle ψ describes the orientation of the polarization axes with respect to the projection of the detectors arms on the sky.

If we define Φ as the orbital phase with respect to the line of ascending nodes (the point at which the orbit crosses the x-y plane from below), then for a circular orbit the polarization states will be given by

$$h_+ = \frac{2\mu}{D}\left(\frac{m}{r}\right)\left\{Q_+ + P^{0.5}Q_+\left(\frac{m}{r}\right)^{1/2} + PQ_+\left(\frac{m}{r}\right) \right.$$
$$\left. + P^{1.5}Q_+\left(\frac{m}{r}\right)^{3/2}\right\}, \qquad (4.28)$$

where the quadrupole term is given by

$$Q_+ = -2\left[C_+\cos 2\Phi + S_+\sin 2\Phi\right], \qquad (4.29)$$

and similarly for $h_\times$ where $+$ is replaced by $\times$, and where

$$C_+ = \tfrac{1}{2}\cos^2\Theta\left(\sin^2\alpha - \cos^2 i\cos^2\alpha\right) + \tfrac{1}{2}(\cos^2 i\sin^2\alpha$$
$$- \cos^2\alpha) - \tfrac{1}{2}\sin^2\Theta\sin^2 i - \tfrac{1}{4}\sin 2\Theta\sin 2i\cos\alpha, \qquad (4.30a)$$

$$S_+ = \tfrac{1}{2}\left(1 + \cos^2\Theta\right)\cos i\sin 2\alpha + \tfrac{1}{2}\sin 2\Theta\sin i\sin\alpha, \qquad (4.30b)$$

$$C_\times = -\tfrac{1}{2}\cos\Theta\sin 2\alpha\left(1 + \cos^2 i\right) - \tfrac{1}{2}\sin\Theta\sin 2i\sin\alpha, \qquad (4.30c)$$

$$S_\times = -\cos\Theta\cos i\cos 2\alpha - \sin\Theta\sin i\cos\alpha, \qquad (4.30d)$$

where (i, α) are the spherical coordinates describing the direction of $\hat{\mathbf{L}}_N$ (see Fig. 2). We give the post-Newtonian corrections to h_+ and $h_\times$ in Appendix B. The evolution of i and α is given by the precession equations (4.17). The evolution of Φ is given by

$$\dot{\Phi} = \omega - \dot{\alpha}\cos i. \qquad (4.31)$$

Note that our expressions for the polarization states (specifically the quadrupole terms) are much more complicated than the expressions in Apostolatos *et al.* [19] because we have defined them with respect to a fixed

coordinate system as opposed to a rotating one. In our description α varies as $\sim \omega_p t$ as the orbit precesses in the case of simple precession. On the other hand, in our description the polarization angle ψ (4.26) (and thus the antenna patterns F_+ and $F_\times$) is constant during the binary's inspiral, while in the description of Ref. [19] it is not. The two descriptions are of course equivalent; we have simply made the complexity of the waveforms more explicit.

From the above equations, it can be seen that the signal in the detector due to the quadrupole waveform can be written as

$$h = C_Q\cos 2\Phi + S_Q\sin 2\Phi, \qquad (4.32)$$

where

$$C_Q = -\frac{4\mu}{D}\left(\frac{m}{r}\right)\left[C_+F_+ + C_\times F_\times\right], \qquad (4.33a)$$

$$S_Q = -\frac{4\mu}{D}\left(\frac{m}{r}\right)\left[S_+F_+ + S_\times F_\times\right]. \qquad (4.33b)$$

The signal can be rewritten as

$$h = A_Q\cos\left[2\Phi - \delta_Q\right], \qquad (4.34)$$

where

$$A_Q = \left\{C_Q^2 + S_Q^2\right\}^{1/2}, \qquad (4.35a)$$

$$\delta_Q = \tan^{-1}\left(S_Q/C_Q\right). \qquad (4.35b)$$

D. Small inclination angles

Let us examine the waveform in the limit of a small inclination angle i. This limit will be valid if the total spin **S** is nearly aligned with the orbital angular momentum **L** or if $|\mathbf{S}| \ll |\mathbf{L}|$. In Fig. 12 we show the region for which the precession angle i is less than 0.2 for an equal mass system. If we expand Eq. (4.29) through $O(i^2)$, the overall signal amplitude due to the quadrupole term (4.35a) will be given by

$$A_Q = \frac{2\mu}{D}\left(\frac{m}{r}\right)\left\{F_+^2(\theta,\phi,\psi)[(1 + \cos^2\Theta)^2 + 2i\sin 2\Theta\left(1 + \cos^2\Theta\right)\cos\alpha - i^2(1 - 2\cos^2\Theta\right.$$
$$+ 5\cos^4\Theta) + 3i^2\sin^2\Theta\left(1 + \cos^2\Theta\right)\cos 2\alpha] + 4F_\times^2(\theta,\phi,\psi)[\cos^2\Theta + i\sin 2\Theta\cos\alpha$$
$$\left. - i^2\cos 2\Theta] + F_+(\theta,\phi,\psi)F_\times(\theta,\phi,\psi)[-2i\sin^3\Theta\sin\alpha + 3i^2\sin^2\Theta\cos\Theta\sin 2\alpha]\right\}^{1/2}. \qquad (4.36)$$

Notice that to lowest order in i the amplitude is constant, independent of the precession angle α, and that the modulations are of $O(i)$ and have the same frequency as the precession frequency, $d\alpha/dt$. For some detector orientations (see below), the $O(i)$ terms are suppressed and the modulations will be of $O(i^2)$ and go as twice the precession frequency.

We can use Eq. (4.36) to explain the features of Fig. 1. Note that this case has been presented in Cutler *et al.*

[15], and in Apostolatos *et al.* [19] for a single detector orientation which corresponds to $\gamma = i$. In Fig. 1, $\Theta = \pi/2$, $F_+ = \cos 2\gamma$, $F_\times = \sin 2\gamma$, and initially $i \approx 0.1$, so that

$$A_Q = \frac{2\mu}{D}\frac{m}{r}\left\{\cos^2 2\gamma\left[1 - i^2 + 3i^2\cos 2\alpha\right]\right.$$
$$\left. - 2i\sin 4\gamma\sin\alpha + 4i^2\sin^2 2\gamma\right\}^{1/2}. \qquad (4.37)$$
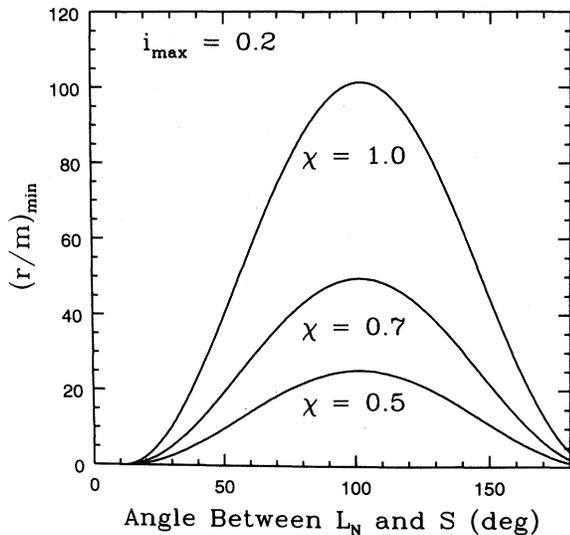
FIG. 12. The region of validity for the small inclination approximation for an equal mass system. The figure plots the minimum separation r/m for which the precession angle i is guaranteed to be less than i_{max} as a function of the angle between $\mathbf{L}$ and $\mathbf{S}$ for several values of the average spin parameter χ of the two bodies. For most neutron star models $\chi \leq 0.7$. Note that at large angles "transitional precession" may occur.

For $\gamma = 0$, the modulations of the amplitude will have a frequency of twice the precession frequency and will be only a few percent ($\approx (3/2)i^2$) of the overall amplitude. For $\gamma = \pi/4$, $A_Q \approx 4i(\mu/D)(m/r)$ which is roughly 20% (initially) of the unmodulated amplitude in the previous case and is unmodulated through $O(i^2)$. The other three cases are modulated by a term with a frequency of twice the precession frequency, and another term with the precession frequency. For $\gamma = \pi/8$, the dominant modulation is of $O(i)$ and varies with the precession frequency. In the other two cases ($\gamma = i/2$ and $\gamma = i$), both modulations are of $O(i^2)$ and contain both α and 2α terms, which leads to their forms in Fig. 1. Finally, let $\gamma = i + \pi/4$. Then $A_Q \approx 8i(\mu/D)(m/r)|\cos(\alpha/2 - \pi/4)|$ which corresponds with Fig. 6 of Ref. [19].

V. RESULTS FOR SPECIFIC SYSTEMS

In this section we will describe several specific cases involving a variety of masses and spins. For some cases, we have solved the equations of motion and precession numerically and used them to calculate the emitted gravitational waveform. In all the examples we will assume the binary's orbit has been circularized prior to entering the frequency bandwidth of a LIGO-type detector.

A. Nonspinning bodies

The case in which neither body is spinning has been studied in previous papers [3–6]. Here we only wish to

mention that if neither body is spinning, the orbital plane remains fixed in space, and the waveform's amplitude increases monotonically (apart from post-Newtonian modulations on orbital time scales; see Fig. 4) as the binary inspirals.

B. Spins perpendicular to the orbital plane

If the spins of the bodies are aligned with the orbital angular momentum, the system evolves in a manner qualitatively similar to the case of nonspinning bodies. Since the spins and orbital angular momentum are aligned, none of them precesses so that the orbital plane remains fixed in space. The only effects the spins will have are a contribution to the orbital phase, and a correction to the amplitude of the waveform.

The contribution to the orbital phase will be important as it affects the accumulated phase of the waveform. Since matched templates will be used to obtain information about the binary from the waveform, any effect which causes the phase to change by one cycle over the thousands in the bandwidth of the detector will be important. If the spin contribution to the phase can be separated from the other contributions, it could be used to make an accurate determination of the spins. However, preliminary studies by Cutler and Flanagan [17] suggest that the spin contribution cannot be separated cleanly from other contributions, but instead are strongly correlated with them, thus making the determination of the individual masses and spins more difficult. Table I compares the spin contribution to the orbital phase with other contributions for various binary systems.

The leading-order correction to the waveform due to the spins is a full post-Newtonian order higher than the quadrupole part of the waveform. Thus it will be small until the late stages of the binary's inspiral. In Fig. 4 we compare the spin contributions to the waveform with other contributions.

C. One spinning body

In the cases in which only one of the bodies is spinning, our numerical results agree with our analytic description of Sec. IV. As the binary inspirals, $\mathbf{L}$ and $\mathbf{S}$ precess about $\mathbf{J}$, with both $\mathbf{L}$ and $\mathbf{J}$ shrinking, and $\mathbf{L}$ tipping away from $\mathbf{J}$ while $\mathbf{S}$ tips toward $\mathbf{J}$ (see Fig. 9). The angle between $\mathbf{L}$ and $\mathbf{S}$ remains constant. $\mathbf{J}$ remains relatively fixed in direction unless $\mathbf{L}$ and $\mathbf{S}$ are nearly antialigned and equal in magnitude, in which case the "transitional precession" described by Apostolatos et al. [19] occurs.

1. Dependence of modulation on detector orientation and location

The precession of the orbital plane causes the waveform amplitude to be modulated since the orientation between the orbital plane and the detector is changing.

The form of this modulation depends on the orientation of the detector and its location with respect to the source. In Fig. 1, which was generated from numerical solutions, we show how the modulation changes for different orientations of a detector at a fixed location. Notice that the size and shape of the modulations vary greatly. These modulations are discussed qualitatively in Sec. IV.

2. Effects of higher-order parts of the waveform

So far, we have just examined how the precession of the orbital plane modulates the dominant quadrupole part of the waveform. The precession will also modulate the amplitude of the post-Newtonian corrections to the waveform. This is illustrated in Fig. 13. Recall that the different contributions to the waveform have different dependences on the orbital phase, so that the overall waveform amplitude is not the sum of the individual higher-order amplitudes. (Note that this is true even without spins.)

D. Two spinning bodies

We are not able to solve the general two-spinning-body problem analytically. We therefore present numerical solutions of the equations of motion and precession. Most cases involving two spinning bodies are qualitatively sim-
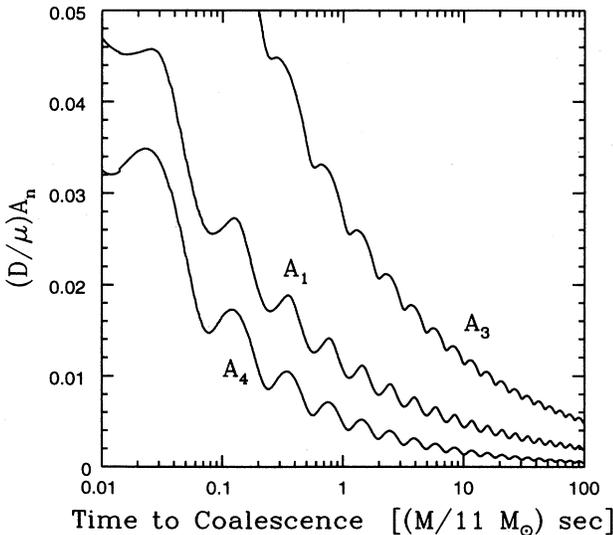
ilar to the case of one spinning body. The main difference lies in the fact that the total spin S is not constant as the spins precess, but rather oscillates between some S_{min} and S_{max}. This causes the angle i between L and J to oscillate as L precesses about J in addition to its overall increase due to gravitational radiation damping. In most cases where spin effects will be important, these oscillations will be small. In each of the following examples, we will examine a pair of inspirals which have the same initial orientation of L and S, but in one case only one of the bodies is spinning, while in the other case both bodies are spinning.

If one of the spins is much smaller than the other, it can be viewed as a perturbation of the simple precession involving the larger spin and the orbital angular momentum. Recall that the spin ratio will go as $|S_1|/|S_2| = (\chi_1/\chi_2)(m_1/m_2)^2$, so that if $m_1 \ll m_2$ and χ_2 is not small, then the spin of the smaller body will be much smaller than that of the larger body, and the above argument will hold. The overall shape of the modulations of the waveform amplitude is the same in both the one spin case and the two spin case. The main difference is that the precession frequency is slightly different in the two cases, which could lead to a noticeable effect on the phase of the waveform. Figure 14 shows the difference in precession rates.

If the masses of the two bodies are equal, Eq. (2.5) implies that the only change in the evolution of S (and thus in $|S|$) compared to the one-spin case will be from the spin-spin coupling. This coupling is weak so that it can be viewed as a perturbation on the simple precession case. Figure 15 illustrates this case. Notice that while the individual spins precess wildly and in effect exchange places, the total spin and orbital angular momentum remain approximately fixed relative to each other ($\kappa \approx$ const). This leads to the overall shape of the modulations of the waveform amplitude to be very similar for the one-spin case
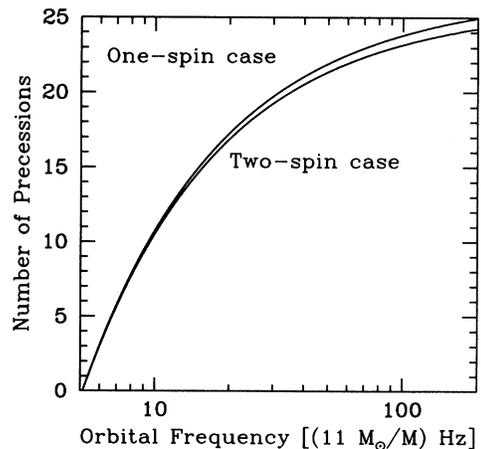

FIG. 13. The amplitude modulations of the higher-order terms of the gravitational waveform. A_1 and A_3 are of $(post)^{1/2}$-Newtonian order beyond the quadrupole term, while A_4 is $(post)^1$-Newtonian order. The quadrupole envelope increase from 0.06 to 0.36 during the portion of the inspiral which is plotted. Note that since the different terms have different dependences on the orbital phase, the overall waveform envelope will not be the sum of the individual envelopes. The binary system is the same as in Fig. 1, but for an observer at $\Theta = \pi/4$, with $\gamma = 0$.

FIG. 14. The rate of precession for the two-spin case and the corresponding one-spin case for a 10:1 mass-ratio system with the total spin S at an angle of $\pi/4$ with the orbital angular momentum L. In the two-spin case, the smaller body's spin is aligned with L. In both cases the bodies are maximally spinning.

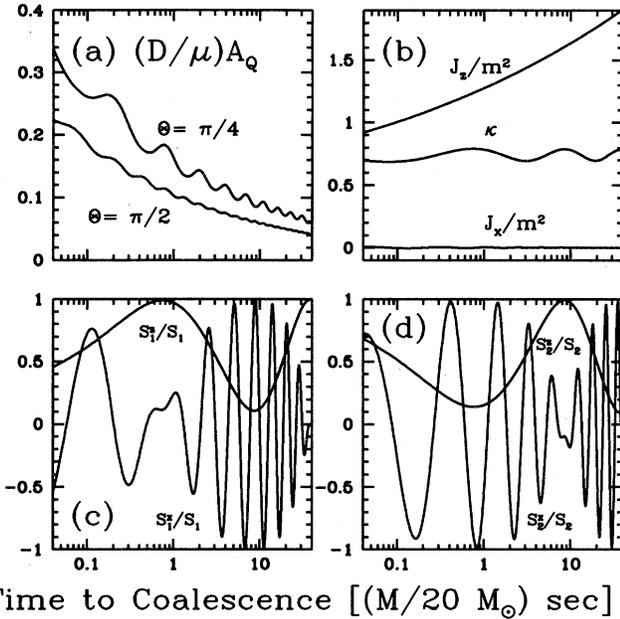Time to Coalescence $[(M/20\ M_\odot)\ \text{sec}]$

FIG. 15. An equal mass case in which the spins of the bodies are equal in magnitude ($\chi_1 = \chi_2 = \sqrt{2}/2$), with one spin aligned with $\mathbf{L}$ and the other perpendicular to it. (a) The modulation of the quadrupole waveform envelope. (b) The components of the total angular momentum $\mathbf{J}$. Notice that $\mathbf{J}$ remains relatively fixed in direction as the binary inspirals due to gravitational radiation emission. Also plotted is the angle between $\mathbf{L}$ and $\mathbf{S}$, which oscillates about a relatively constant value. (c) The components of $\mathbf{S}_1$. (d) The components of $\mathbf{S}_2$. Notice that while the individual spins undergo substantial precessions, the total spin precesses in a fairly simple manner. This causes the two-spin case to be similar to the corresponding one-spin case.

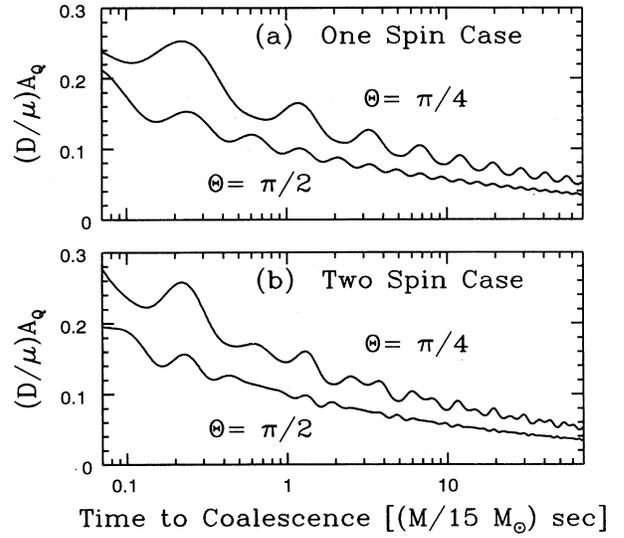

Time to Coalescence $[(M/15\ M_\odot)\ \text{sec}]$

FIG. 16. The modulation of the quadrupole waveform envelope for a 2:1 mass-ratio system with the total spin $\mathbf{S}$ initially perpendicular to $\mathbf{L}$. (a) One spinning body. (b) Two spinning bodies with spins equal such that the smaller body's spin is maximal ($\chi = 1$). Note the substantial differences in the modulations between the two cases. This is a result of the complicated precession when both bodies are spinning. See Figs. 9 and 10 for a depiction of the precession of the orbital angular momentum for these cases.

and the two-spin case. As in the previous example there is a difference in the precession frequency between the two cases, which could lead to a noticeable effect on the phase of the waveform.

In some cases, however, the oscillations in i can be significant, and cannot be viewed as a perturbation of a simple precession case. Figure 16 illustrates this case, for equal spins but different masses. Even though the spins are equal in magnitude, the different masses will cause them to precess at different rates [see Eq. (2.5)]. At some times the two spins will align and i will be at its largest value. At other times the two spins will almost cancel each other, and $\mathbf{L}$ will be aligned with $\mathbf{J}$. Thus the orbital plane will tilt back and forth as it precesses about $\mathbf{J}$. This leads to substantial differences between the two-spin case and the one-spin case, as illustrated by the complex modulations in Fig. 16.

Another case in which the second spin will be important is that of "transitional precession" described by Apostolatos et al. [19]. Recall that in this case $\mathbf{L}$ and $\mathbf{S}$ almost cancel each other, so that any perturbations in $\mathbf{S}$ will cause noticeable effects. See Ref. [19] for more details.

VI. CONCLUSIONS

In this paper we have examined the importance of spin-orbit and spin-spin effects on the inspiral of a coalescing binary system of compact objects and on the gravitational radiation emitted from such a system. The inclusion of spin effects makes the study of coalescing binary systems much more complicated because of the extra degrees of freedom for the orbit, and the extra parameters upon which the waveform will depend. On the other hand, if the effects due to the spins can be separated from other post-Newtonian effects, more information about the binary system can be extracted from the observed waveforms.

The spins of the bodies have two major effects on the inspiral of the binary. As long as the spins are not perpendicular to the orbital plane, the orbital plane will precess, thus changing its orientation in space. In most cases, this precession will be a relatively simple precession of the orbital angular momentum $\mathbf{L}$ about the total angular momentum $\mathbf{J}$. In some cases, however, the precession can be quite complicated (see Sec. II). In addition to the precession effect, the spins will contribute to the evolution of the orbital phase, in the same manner that other post-Newtonian terms contribute (see Sec. IV and Table I). The spin-orbit contribution can be of the same magnitude as the post-Newtonian and leading-order tail contributions to the orbital phase. The spin-spin contribution, on the other hand, is quite small. These contributions to

the orbital phase will change the rate of inspiral.

The spins will change the amplitude of the observed waveform in several ways. The major effect the spins have is due to the precession of the orbital plane. This causes the orientation of the orbit to be changed with respect to the detector, which results in modulation of the amplitude of the waveform (see Sec. IV and Fig. 1). The size and shape of the modulations are sensitive to the location of the detector with respect to the binary system and to the orientation of the detector arms. The spins also directly contribute to the amplitude of the waveform in the same manner that other higher post-Newtonian terms contribute (see Sec. III and Fig. 4). The direct spin contribution to the amplitude may be difficult to detect because it is much smaller than the quadrupole term and the leading-order post-Newtonian terms until very late in the inspiral. The modulations due to precession, however, will be quite noticeable in many cases involving spinning bodies.

The spins will also affect the phase of the observed waveform in several ways. Since the spins affect the evolution of the orbital phase, this will in turn affect the evolution of the phase of the gravitational waveform since it is related to the orbital phase. The phase will also be affected by the precession of the orbital plane since the point from which the orbital phase is measured is itself moving (see Sec. IV). These two effects are independent of one another as one may be present without the other. These effects are very important, however, as the sensitivity with which the phase of the waveform can be measured is currently thought to be the best way of extracting information about the binary system.

In general, the effects of the spins on the waveform amplitude will be small for the case of two coalescing neutron stars. One reason is that for the majority of the time in which the frequency of the gravitational waves from the binary are in the bandwidth of a LIGO-type detector, the orbital angular momentum will be much larger than the spin angular momentum. For example, over 95% of the gravitational wave cycles will occur between $r = 174m$ and $r = 37m$ for two $1.4M_\odot$ neutron stars, and as Fig. 3 shows, $\mathbf{L}$ is at least 5 times larger than $\mathbf{S}$. This means that the inclination angle i will be small throughout most, if not all, of the observed inspiral. This implies that the small inclination angle approximation will hold, so that the amplitude modulations will be on the order of i. For small enough i, one might be able to ignore the modulations to first order and treat the orbital plane to be fixed perpendicular to $\mathbf{J}$ (which is relatively fixed) instead of $\mathbf{L}$ (which is precessing). Then the modulations can be treated as perturbations of $O(i)$.

While the modulations of the amplitude of the waveform may be small, the spin effects on the phase of the waveform are significant for a coalescing binary system of neutron stars. While the spin-orbit contribution to the orbital phase is less than one percent of the total (see Table I), a neutron star with $\chi = S_{NS}/m_{NS}^2$ as small as 0.01 can cause the accumulated gravitational wave phase to change by a cycle from an equivalent system with no spins over the bandwidth of 10 Hz to 1000 Hz. A further contribution to the waveform's phase will come from the precession of the orbital plane. This contribution should vary at the precession frequency. Since $\mathbf{L} \gg \mathbf{S}$ for a binary neutron star coalescence, we may substitute $\mathbf{L}$ for $\mathbf{J}$ in Eq. (2.14) and integrate over the inspiral, finding that the binary precesses roughly 60–70 times over the detector's bandwidth of 10 Hz to 1000 Hz.

Spin effects can be very important for coalescing binary systems with a very massive black hole and a neutron star. Since the spins can dominate the orbital angular momentum, large precession angles are possible, leading to very large amplitude modulations. Furthermore, the spin-orbit contribution to the orbital phase is a larger percentage of the total.

We have examined how the spins of the body affect the inspiral of the binary system and the gravitational radiation emitted therefrom. There are many interesting questions that remain to be examined. One is the inverse problem: Given an observed waveform, how much information about the spins of the bodies can be extracted? A related question is, how much will spin effects complicate the extraction of the masses and other information from the waveform? Preliminary studies by Cutler and Flanagan [17] indicate that the spin-orbit contribution to the orbital phase will be difficult to separate from the post-Newtonian contribution which is used to determine the mass ratio because of their similar dependences on (m/r) or $(m\omega)$ in the evolution of the phase [see Eq. (4.16)]. Further studies are needed to determine whether Newtonian templates without explicit spin contributions to the waveforms can be used on systems which have spins without significant loss of signal-to-noise ratio. If not, then the number of templates which will be needed to study coalescing binary systems of compact objects will increase significantly.

ACKNOWLEDGMENTS

APPENDIX A: SPIN SUPPLEMENTARY CONDITIONS

When examining systems containing spinning bodies, it is important to note that the form of the spin-orbit acceleration $\mathbf{a}_{SO}$ is not unique, but rather depends on a "spin supplementary condition" (SSC). For example, three different forms of $\mathbf{a}_{SO}$,

$$\mathbf{a}_{\text{SO}}^{(\text{I})} = \frac{1}{r^3}\left\{6\hat{\mathbf{n}}\left[(\hat{\mathbf{n}}\times\mathbf{v})\cdot\left(2\mathbf{S}+\frac{\delta m}{m}\mathbf{\Delta}\right)\right]\right.$$
$$-\left[\mathbf{v}\times\left(7\mathbf{S}+3\frac{\delta m}{m}\mathbf{\Delta}\right)\right]$$
$$\left.+3\dot{r}\left[\hat{\mathbf{n}}\times\left(3\mathbf{S}+\frac{\delta m}{m}\mathbf{\Delta}\right)\right]\right\}, \qquad (\text{A1a})$$

$$\mathbf{a}_{\text{SO}}^{(\text{II})} = \frac{1}{r^3}\left\{\frac{3}{2}\hat{\mathbf{n}}\left[(\hat{\mathbf{n}}\times\mathbf{v})\cdot\left(7\mathbf{S}+3\frac{\delta m}{m}\mathbf{\Delta}\right)\right]\right.$$
$$-\left[\mathbf{v}\times\left(7\mathbf{S}+3\frac{\delta m}{m}\mathbf{\Delta}\right)\right]$$
$$\left.+\frac{3}{2}\dot{r}\left[\hat{\mathbf{n}}\times\left(7\mathbf{S}+3\frac{\delta m}{m}\mathbf{\Delta}\right)\right]\right\}, \qquad (\text{A1b})$$

$$\mathbf{a}_{\text{SO}}^{(\text{III})} = \frac{1}{r^3}\left\{3\hat{\mathbf{n}}\left[(\hat{\mathbf{n}}\times\mathbf{v})\cdot\left(3\mathbf{S}+\frac{\delta m}{m}\mathbf{\Delta}\right)\right]\right.$$
$$-\left[\mathbf{v}\times\left(7\mathbf{S}+3\frac{\delta m}{m}\mathbf{\Delta}\right)\right]$$
$$\left.+6\dot{r}\left[\hat{\mathbf{n}}\times\left(2\mathbf{S}+\frac{\delta m}{m}\mathbf{\Delta}\right)\right]\right\}, \qquad (\text{A1c})$$

are given by the three different SSC's;

$$S_A^{\mu\nu}u_{A\nu} = 0, \qquad (\text{A2a})$$

$$2S_{Ai0} + S_{Aij}v_A^j = 0, \qquad (\text{A2b})$$

$$S_A^{i0} = 0, \qquad (\text{A2c})$$

respectively, where u_A^μ is the four-velocity of the center-of-mass world line X_A^μ of body A, and

$$S_A^{\mu\nu} \equiv 2\int_A (x^{[\mu} - X_A{}^{[\mu})\tau^{\nu]0}d^3x, \qquad (\text{A3})$$

where $\tau^{\mu\nu}$ denotes the stress-energy tensor of matter plus gravitational fields satisfying $\tau^{\mu\nu}{}_{,\nu} = 0$, and square brackets around indices denote antisymmetrization. Note that the spin vector $\mathbf{S}$ of each body is defined by $S_A^i = \frac{1}{2}\epsilon_{ijk}S_A^{jk}$.

Barker and O'Connell [27] showed that these different forms of $\mathbf{a}_{\text{SO}}$ are equivalent if one takes into account that the different SSC's are related to different locations $\mathbf{X}_A$ of the center of mass of each body. Furthermore, they found transformations from the center-of-mass definition given by one SSC to that of another. For example

$$X_A^{i\,(\text{II})} \longrightarrow X_A^{i\,(\text{I})} + \frac{1}{2m_A}\left(\mathbf{v}_A\times\mathbf{S}_A\right)^i. \qquad (\text{A4})$$

This shift in the center-of-mass world line is of post-Newtonian order, and so it can be neglected at lowest order.

In Sec. II, we chose to use the form of $\mathbf{a}_{\text{SO}}$ given by the first SSC (A2a), since it is covariant. In doing so, we have chosen a center-of-mass definition through the

SSC, and we must insure that any future center-of-mass definitions we use are consistent with this choice. In Sec. III, we use an integral definition of the center of mass of each body,

$$x_A^i = \frac{1}{m_A}\int_A x^i\rho^*(\mathbf{x})\left[1 + \frac{1}{2}\bar{v}_A^2 + \Pi - \frac{1}{2}\bar{U}_A\right]d^3x, \quad (\text{A5})$$

to evaluate the BDI multipoles, where

$$m_A = \int_A \rho^*(\mathbf{x})\left[1 + \frac{1}{2}\bar{v}_A^2 + \Pi - \frac{1}{2}\bar{U}_A\right]d^3x, \qquad (\text{A6})$$

where $\bar{v}_A^i = v^i - v_A^i$, $v_A^i = dx_A^i/dt$, and $\bar{U}_A$ is the Newtonian potential produced by the Ath body itself. This is a "natural" post-Newtonian definition since it uses the total mass, kinetic energy, internal energy, and gravitational potential energy of each body as the weighting factor. However, it turns out that this definition of the center of mass is not related to the first SSC which we chose for our equations of motion, but rather to the second SSC (A2b). This can be seen by the following argument.

It is straightforward to show that the three SSC's can be rewritten in the form

$$S_A^{i0} - kS_A^{ij}v_A^j = 0, \qquad (\text{A7})$$

where $k = 1$ for the first SSC, $k = 1/2$ for the second, and $k = 0$ for the third. From Eq. (A3) we see that

$$S_A^{i0} = \int_A (x^i - X_A^i)\tau^{00}d^3x, \qquad (\text{A8})$$

since the integration is done at constant time. It is straightforward to show that, to post-Newtonian order,

$$\tau^{00} = (1 + 4U)T^{00} - \frac{7}{8\pi}|\nabla U|^2. \qquad (\text{A9})$$

Substituting Eq. (A9) into Eq. (A8) and integrating the $|\nabla U|^2$ terms by parts, we obtain

$$S_A^{i0} = \int_A \rho^*(\mathbf{x})(x^i - X_A^i)\left[1 + \frac{1}{2}v^2 - \frac{1}{2}U + \Pi\right]d^3x. \qquad (\text{A10})$$

Using our integral definition of the mass and center of mass of body A (A5), we obtain

$$S_A^{i0} = m_A x_A^i\left(1 + \frac{1}{2}v^2 - \frac{1}{2}\sum_B \frac{m_B}{r_{AB}}\right) + \frac{1}{2}v_A^j S_A^{ij}$$
$$-m_A\left(1 + \frac{1}{2}v^2 - \frac{1}{2}\sum_B \frac{m_B}{r_{AB}}\right)X_A^i. \qquad (\text{A11})$$

Thus our integral definition of the center of mass corresponds to the SSC definition $(x_A^i = X_A^i)$, if $S^{i0} = \frac{1}{2}v_A^j S^{ij}$, i.e., the second SSC. Imposing the general SSC (A7) on Eq. (A11), we see that, to post-Newtonian order,

$$x_A^i = X_A^{i\,(k)} + \frac{2k-1}{2m_A}S_A^{ij}v_A^j. \qquad (\text{A12})$$

Thus in order that the center of mass used in the STF moments be consistent with that used in the equations of motion, we must transform from $x_A^i = X_A^{i(\text{II})}$ to $X_A^{i(\text{I})}$ in the moments by using Eq. (A4) (see Sec. III).

This is also consistent with Brumberg [11] who derived the equations of motion from our integral definition of the center of mass, and found the form of $\mathbf{a}_{SO}$ to be that of the second SSC without ever having mentioned the concept of an SSC.

Another check of the consistency of our argument is seen by evaluating the BDI mass dipole moment [23,24], given by

$$I^i = \sum_A \left\{ \int_A x^i \rho^*(\mathbf{x}) \left[1 + \frac{1}{2}v^2 - \frac{1}{2}U + \Pi \right] d^3x \right\}. \quad \text{(A13)}$$

Evaluating the integral in the manner used to evaluate the mass quadrupole (in Sec. III), we obtain

$$I^i = \sum_A \left\{ m_A x_A^i \left[1 + \frac{1}{2}v_A^2 - \frac{1}{2} \sum_{B \neq A} \frac{m_B}{r_{AB}} \right] \right.$$

$$\left. + \frac{1}{2} \left(\mathbf{v}_A \times \mathbf{S}_A \right)^i \right\}, \quad \text{(A14)}$$

where we have dropped the post-Newtonian terms as they do not affect the calculation. We then use Eq. (A4) to shift the center of mass x_A^i from that defined by the second SSC $X_A^{i(\text{II})}$ to that of our equations of motion, $X_A^{i(\text{I})}$. The result is

$$I^i = \sum_A \left\{ m_A x_A^i \left[1 + \frac{1}{2}v_A^2 - \frac{1}{2} \sum_{B \neq A} \frac{m_B}{r_{AB}} \right] \right.$$

$$\left. + \left(\mathbf{v}_A \times \mathbf{S}_A \right)^i \right\}, \quad \text{(A15)}$$

where x_A^i now refers to $X_A^{i(\text{I})}$. Blanchet and Damour [23] have proved on general grounds that

$$\frac{d^2}{dt^2} I_i = 0. \quad \text{(A16)}$$

Taking two time derivatives of Eq. (A15) and substituting our equations of motion where appropriate, we verify that Eq. (A16) does hold. [Alternatively, we could have taken two time derivatives of the mass dipole before shifting the center of mass of each body and seen that $\mathbf{a}_{SO}^{\text{II}}$ is needed to ensure that Eq. (A16) holds.]

APPENDIX B: POST-NEWTONIAN CORRECTIONS TO THE WAVEFORM FOR A CIRCULAR ORBIT

If we define Φ as the orbital phase with respect to the line of ascending nodes (the point at which the orbit crosses the x-y plane from below), then for a circular orbit the polarization states will be given by

$$h_+ = \frac{2\mu}{D} \left(\frac{m}{r} \right) \left\{ Q_+ + P^{0.5}Q_+ \left(\frac{m}{r} \right)^{1/2} + PQ_+ \left(\frac{m}{r} \right) \right\}, \quad \text{(B1)}$$

where, for simplicity we include only the post-Newtonian terms through PQ_+, and

$$Q_+ = -2 \left[C_+ \cos 2\Phi + S_+ \sin 2\Phi \right], \quad \text{(B2a)}$$

$$P^{0.5}Q_+ = \frac{1}{4} \frac{\delta m}{m} \left[9 \left(aS_+ + bC_+ \right) \cos 3\Phi + 9 \left(bS_+ - aC_+ \right) \sin 3\Phi \right.$$

$$\left. + \left(3aS_+ - 3bC_+ - 2bK_+ \right) \cos \Phi - \left(3bS_+ + 3aC_+ - 2aK_+ \right) \sin \Phi \right], \quad \text{(B2b)}$$

$$PQ_+ = \frac{8}{3}(1 - 3\eta) \left\{ \left[(a^2 - b^2)C_+ - 2abS_+ \right] \cos 4\Phi + \left[(a^2 - b^2)S_+ + 2abC_+ \right] \sin 4\Phi \right\}$$

$$+ DC_+ \cos \Phi + DS_+ \sin \Phi + \frac{1}{6} \left\{ \left[4(1 - 3\eta)(a^2 + b^2) + (19 - 3\eta) \right] Q_+ \right.$$

$$\left. - 4(1 - 3\eta) \left[(a^2 - b^2) \cos 2\Phi + 2ab \sin 2\Phi \right] K_+ \right\}, \quad \text{(B2c)}$$

and similarly for $h_\times$ where $+$ is replaced by $\times$, and where

$$C_+ = \frac{1}{2} \cos^2 \Theta \left(\sin^2 \alpha - \cos^2 i \cos^2 \alpha \right) + \frac{1}{2}(\cos^2 i \sin^2 \alpha$$

$$- \cos^2 \alpha) - \frac{1}{2} \sin^2 \Theta \sin^2 i - \frac{1}{4} \sin 2\Theta \sin 2i \cos \alpha, \quad \text{(B3a)}$$

$$S_+ = \frac{1}{2} \left(1 + \cos^2 \Theta \right) \cos i \sin 2\alpha + \frac{1}{2} \sin 2\Theta \sin i \sin \alpha, \quad \text{(B3b)}$$

$$K_+ = \frac{1}{2} \cos^2 \Theta \left(\sin^2 \alpha + \cos^2 i \cos^2 \alpha \right) - \frac{1}{2}(\cos^2 i \sin^2 \alpha$$

$$+ \cos^2 \alpha + \frac{1}{2} \sin^2 \Theta \sin^2 i + \frac{1}{4} \sin 2\Theta \sin 2i \cos \alpha, \quad \text{(B3c)}$$

$$DC_+ = -\frac{1}{m^2} \left[\Delta^y \sin \alpha \cos \Theta + d \cos \alpha \right], \quad \text{(B3d)}$$

$$DS_+ = -\frac{1}{m^2} \left[c\Delta^y - d \cos i \sin \alpha \right], \quad \text{(B3e)}$$

$$C_\times = -\tfrac{1}{2}\cos\Theta\sin2\alpha\left(1+\cos^2 i\right) - \tfrac{1}{2}\sin\Theta\sin2i\sin\alpha, \tag{B3f}$$

$$S_\times = -\cos\Theta\cos i\cos2\alpha - \sin\Theta\sin i\cos\alpha, \tag{B3g}$$

$$K_\times = -\tfrac{1}{2}\cos\Theta\sin2\alpha\sin^2 i + \tfrac{1}{2}\sin\Theta\sin2i\sin\alpha, \tag{B3h}$$

$$DC_\times = \frac{1}{m^2}\left[\Delta^y\cos\alpha - d\cos\Theta\sin\alpha\right], \tag{B3i}$$

$$DS_\times = \frac{1}{m^2}\left[-\Delta^y\cos i\sin\alpha + cd\right], \tag{B3j}$$

$$a = -\sin\Theta\sin\alpha, \tag{B3k}$$

$$b = \cos\Theta\sin i - \sin\Theta\cos i\cos\alpha, \tag{B3l}$$

$$c = \cos\Theta\cos i\cos\alpha + \sin i\sin\Theta, \tag{B3m}$$

$$d = \Delta^z\sin\Theta - \Delta^x\cos\Theta, \tag{B3n}$$

where (i,α) are the spherical coordinates describing the direction of $\hat{\mathbf{L}}_N$ (see Fig. 2).

From the above equations, it can be seen that the signal in the detector can be written as a series

$$h = \sum_{n=1}^{2(N+1)}\left\{C_n\cos n\Phi + S_n\sin n\Phi\right\}, \tag{B4}$$

which can be rewritten as

$$h = \sum_{n=1}^{2(N+1)} A_n\cos\left[n\Phi - \delta_n\right], \tag{B5}$$

where

$$A_n = \left\{C_n^2 + S_n^2\right\}^{1/2}, \tag{B6a}$$

$$\delta_n = \arctan\left(S_n/C_n\right), \tag{B6b}$$

and N is the final post-Newtonian order beyond the quadrupole term to which the waveform is calculated. For example, if we look at only the quadrupole contribution to the waveform, then only the $n = 2$ terms will be nonzero and

$$C_2 = -\frac{4\mu}{D}\left(\frac{m}{r}\right)\left[C_+F_+ + C_\times F_\times\right], \tag{B7a}$$

$$S_2 = -\frac{4\mu}{D}\left(\frac{m}{r}\right)\left[S_+F_+ + S_\times F_\times\right]. \tag{B7b}$$

From Eqs. (B2) we see that the post-Newtonian corrections to the waveform depend on different harmonics of the orbital frequency than the quadrupole term. Eq. (B5) splits the signal into the terms depending on the different harmonics. Each term will have its amplitude modulated by the precession of the orbital plane.

APPENDIX C: A COMPARISON WITH TEST-MASS CALCULATIONS

Recently, Poisson [34] has calculated the gravitational waveform and energy loss due to gravitational radiation from a particle in a circular, equatorial orbit around a slowly rotating black hole. Poisson's calculations were done using the Teukolsky perturbation formalism, which is completely different from the post-Newtonian calculations we used. In this appendix, we show that our results for the waveform and energy loss agree with those of Poisson in the appropriate limit. Since we are only interested in the spin-orbit terms, we will neglect all the other post-Newtonian terms.

Poisson gives the energy loss as

$$\frac{dE}{dt} = -\frac{32}{5}\left(\frac{\mu}{m}\right)^2(m\omega)^{10/3}\left[1 - \frac{11}{4}\chi_{BH}(m\omega)\right] \tag{C1}$$

and the spin-orbit contributions to the waveform as

$$h_+ = \frac{2\mu}{D}(m\omega)^{2/3}\left\{Q_+ - \chi_{BH}\left[\sin\Theta\sin\Phi(m\omega)^{2/3}\right.\right.$$
$$\left.\left. - \frac{4}{3}\left(1+\cos^2\Theta\right)\cos2\Phi(m\omega)\right]\right\}, \tag{C2a}$$

$$h_\times = \frac{2\mu}{D}(m\omega)^{2/3}\left\{Q_\times + \chi_{BH}\left[\sin\Theta\cos\Theta\cos\Phi(m\omega)^{2/3}\right.\right.$$
$$\left.\left. + \frac{8}{3}\cos\Theta\sin2\Phi(m\omega)\right]\right\}, \tag{C2b}$$

where we have rewritten the equations using our notation.

Combining Eqs. (4.10) and (4.13) we find the energy loss to be

$$\frac{dE}{dt} = -\frac{32}{5}\eta^2(m\omega)^{10/3}\left\{1 - \frac{1}{4}\sum_{i=1,2}\chi_i(\hat{\mathbf{L}}_N\cdot\hat{\mathbf{s}}_i)\right.$$
$$\left.\times\left(11\frac{m_i^2}{m^2} + 5\eta\right)(m\omega)\right\}. \tag{C3}$$

In the test-mass limit that we are considering, $m_1 = \mu$, $m_2 = m$ (with $\mu \ll m$), $\eta = \mu/m$, $\chi_1 = 0$, $\chi_2 = \chi_{BH}$, $\delta m = -m$, $\hat{\mathbf{s}}_2 = \hat{\mathbf{L}}_N$, and $\boldsymbol{\Delta} = \chi_{BH}m^2\hat{\mathbf{L}}_N$. Substituting these values into Eq. (C3) we see that our expression for the energy loss agrees with that of Poisson in the appropriate limit.

Combining Eqs. (4.8) and (4.13) and taking the above test-mass limit of the spin contributions yields

$$h_c^{ij} = \frac{2\mu}{D}(m\omega)^{2/3}\left\{Q_c^{ij} + 2\chi_{BH}(m\omega)^{2/3}n^{(i}(\hat{\mathbf{L}}\times\hat{\mathbf{N}})^{j)}\right.$$
$$\left. + \frac{8}{3}\chi_{BH}(m\omega)\left[n^i n^j - \lambda^i\lambda^j\right]\right\}. \tag{C4}$$

Substituting $\hat{\mathbf{n}} = \cos\Phi\hat{\mathbf{x}} + \sin\Phi\hat{\mathbf{y}}$ and $\hat{\boldsymbol{\lambda}} = -\sin\Phi\hat{\mathbf{x}} + \cos\Phi\hat{\mathbf{y}}$ into the above expression and inserting the results into Eqs. (4.23), we obtain a result which matches that of Poisson.

[1] A. Abramovici, W. E. Althouse, R. W. P. Drever, Y. Gürsel, S. Kawamura, F. J. Raab, D. Shoemaker, L. Sievers, R. E. Spero, K. S. Thorne, R. E. Vogt, R. Weiss, S. E. Whitcomb, and M. E. Zucker, Science **256**, 325 (1992); B. F. Schutz, Class. Quantum Grav. **6**, 1761 (1989).

[2] J. H. Taylor, A. Wolszczan, T. Damour, and J. M. Weisberg, Nature (London) **355**, 132 (1992).

[3] C. W. Lincoln and C. M. Will, Phys. Rev. D **42**, 1123 (1990).

[4] A. G. Wiseman, Phys. Rev. D **46**, 1517 (1992).

[5] L. E. Kidder, C. M. Will, and A. G. Wiseman, Phys. Rev. D **47**, 3281 (1993).

[6] A. G. Wiseman, Phys. Rev. D **48**, 4757 (1993).

[7] L. Blanchet, T. Damour, B. R. Iyer, C. M. Will, and A. G. Wiseman, Phys. Rev. Lett. **74**, 3515 (1995).

[8] B. M. Barker and R. F. O'Connell, Gen. Relativ. Gravit. **11**, 149 (1979).

[9] K. S. Thorne and J. B. Hartle, Phys. Rev. D **31**, 1815 (1985).

[10] For a thorough review, see T. Damour, in *300 Years of Gravitation*, edited by S. Hawking and W. Israel (Cambridge University Press, Cambridge, 1987), p. 128.

[11] V. A. Brumberg, *Essential Relativistic Celestial Mechanics* (Adam Hilger, Bristol, 1991), p. 155.

[12] C. S. Kochanek, Astrophys. J. **398**, 234 (1992); L. Bildsten and C. Cutler, *ibid.* **400**, 175 (1992).

[13] L. E. Kidder, C. M. Will, and A. G. Wiseman, Phys. Rev. D **47**, R4183 (1993).

[14] L. E. Kidder, C. M. Will, and A. G. Wiseman, Class. Quantum Grav. Lett. **9**, L125 (1992).

[15] C. Cutler, T. A. Apostolatos, L. Bildsten, L. S. Finn, E. E. Flanagan, D. Kennefick, D. M. Markovic, A. Ori, E. Poisson, G. J. Sussman, and K. S. Thorne, Phys. Rev. Lett. **70**, 2984 (1993).

[16] L. S. Finn (private communication).

[17] C. Cutler and E. E. Flanagan, Phys. Rev. D **49**, 2658 (1994).

[18] J. L. Friedman and J. R. Ipser, Philos. Trans. R. Soc. London **A340**, 391 (1992).

[19] T. A. Apostolatos, C. Cutler, G. J. Sussman, and K. S. Thorne, Phys. Rev. D **49**, 6274 (1994).

[20] B. R. Iyer and C. M. Will, Phys. Rev. Lett. **70**, 116 (1993); B. R. Iyer and C. M. Will (in preparation).

[21] T. Damour and N. Deruelle, C. R. Acad. Sci. Paris **293**, 537 (1981); **293**, 877 (1981); T. Damour, in *Gravitational Radiation*, edited by N. Deruelle and T. Piran (North-Holland, Amsterdam, 1983), p. 59; L. P. Grishchuk and S. M. Kopejkin, in *Relativity in Celestial Mechanics and Astrometry*, edited by J. Kovalevsky and V. A. Brumberg (Reidel, Dordrecht, 1986), p. 19.

[22] K. S. Thorne, Rev. Mod. Phys. **52**, 299 (1980).

[23] L. Blanchet and T. Damour, Ann. Inst. Henri Poincaré A, **50**, 377 (1989).

[24] T. Damour and B. R. Iyer, Ann. Inst. Henri Poincaré **54**, 115 (1991).

[25] See, for example, C. M. Will, *Theory and Experiment in Gravitational Physics* (Cambridge University Press, Cambridge, England, 1981), p. 111.

[26] L. Blanchet and G. Schäfer, Mon. Not. R. Astron. Soc. **239**, 845 (1989).

[27] B. M. Barker and R. F. O'Connell, Gen. Relativ. Gravit. **5**, 539 (1974).

[28] T. Damour and N. Deruelle, C. R. Acad. Sci. Paris **293**, 877 (1981).

[29] L. Blanchet and T. Damour, Phys. Rev. D, **46**, 4304 (1992).

[30] R. V. Wagoner and C. M. Will, Astrophys. J. **210**, 764 (1976); **215**, 984 (1977).

[31] W. Junker and G. Schäfer, Mon. Not. R. Astron. Soc. **254**, 146 (1992).

[32] M. J. Fitchett, Mon. Not. R. Astron. Soc. **203**, 1049 (1983).

[33] L. S. Finn and D. F. Chernoff, Phys. Rev. D **47**, 2198 (1993).

[34] E. Poisson, Phys. Rev. D **48**, 1860 (1993).